A FINITE ELEMENT MODEL

OF THE SUPERIOR GLENOID LABRUM

by

Eunjoo Hwang

A dissertation submitted in partial fulfillment
of the requirements for the degree of
Doctor of Philosophy
(Kinesiology and Biomedical Engineering)
in the University of Michigan
2014

Doctoral Committee:

Assistant Professor Mark L. Palmer, Co-Chair
Professor Emeritus John A. Faulkner, Co-Chair
Research Professor James A. Ashton-Miller
Associate Professor James E. Carpenter
Associate Professor Richard E. Hughes

ACKNOWLEDGMENTS

I would like to thank my thesis committee for the help they have provided. In particular, times with my co-advisors, Dr. Mark L. Palmer, and Dr. John A. Faulkner, have influenced my life and work. I thank Dr. Palmer for his continual guidance and his invaluable assistance with practical and theoretical issues. My experiences and my scope have been expanded by working with Dr. Palmer. I also would like to thank Dr. Faulkner for his inspiration and his guidance. After working with Dr. Faulkner, I am heartened in this journey. In all obstacles which I encountered in my research he always has encouraged me to move forward. I wish to thank Dr. James Ashton-Miller for his intellectual input covering a wide range of fields. With his essential, and insightful comments, I could research and present findings effectively. I am sincerely thankful to Dr. James Carpenter for his tremendous contribution to the clinical aspects of this work. With his expert knowledge of clinical issues, clinical relevance was taken into consideration for the current study. I am extremely grateful to Dr. Richard Hughes for his priceless guidance, mentorship, and support. From him, I learned the requisite skills for being a well-trained, productive researcher in a group. I profoundly appreciate their time, which they have taken to help in my development as a scientist.

I want to express my gratitude to several individuals for their specific contributions as I worked toward a degree in the individual interdepartmental program. Thanks to the approval by Dr. Rod Fort, I could initiate this program. I also would like to thank Dr. Ketra Armstrong and

Dr. Melissa Gross for their warm encouragement, thoughtful guidance, and important feedback on the research. Dr. Daniel Ferris, Dr. Susan Brooks, and Dr. Christopher Mendias helped me to acquire knowledge of both Movement Science and Biomechanical engineering field. I thank Charlene Ruloff, Maria Steele, and Leona Cranford for their great help and readiness to answer any and all questions.

I am blessed with excellent coworkers in multiple labs (the Musculoskeletal Tissue Emulation Lab, the Orthopaedic Research Lab, Muscle Mechanics Lab and the radiology lab). I thank Dr. Jon Jacobson for his practical contribution of MRIs. I really appreciate Ms. Carol Davis, and Ms. Jane Heibel for their endless support in both administrative and practical fields. I acknowledge Tom Cichonski for his great support on preparing and submitting manuscripts to the specific journal. Thanks to Dr. Chris Gatti, this study could be started. Erin Bigelow, Alexander Brunfeldt, Charles Roehm, and Suzan Lowe provided technical assistance in obtaining anatomical images of the shoulder specimen. I thank Zeeshan Ahmed for his assistant about modeling and Rory Stephen Crook for his willingness to help. Short conversations with Dan Holland and Dr. Jesal Parekh refreshed me.

I would like to acknowledge my friends with my gratitude for their prayers and support. Professors and scholars in the Korea University and Korean Institute of Machinery and Materials supported my choice to start this new field. My lifelong friends from the University of Michigan, Korea University, Korean leadership school, and high school encouraged me with their prayers. My parents-in-law and brother-in-law are so understanding and helping me to focus on study. My parents and sister have stood by my side and prayed for God's hands in my life. Thanks to these people in my life, I can get back up when I fall.

Without the warm encouragement, loving support, and endless patience by my wonderful husband, Gu, my sweet daughter, Emanuela, and my God, none of this would have been possible. I would like to thank God for opportunity to praise him through my work and life.

TABLE OF CONTENTS

LIST OF FIGURES

ABSTRACT

A FINITE ELEMENT MODEL OF THE SUPERIOR GLENOID LABRUM

by

Eunjoo Hwang

Co-chairs: Mark L. Palmer and John A. Faulkner

Despite numerous studies on the function and pathologies of the shoulder joint's superior glenoid labrum, controversy still exists concerning the mechanism of injury to the superior labral in the anterior to posterior direction (SLAP), and thus the optimal treatment. In this dissertation, the working hypothesis was that it is possible to use finite element models to explore the factors underlying the initiation and propagation of a SLAP lesion. First, the finite element model was validated for studying the tear mechanism in the superior labrum. An area of high strain correlated well with the location of SLAP tears observed clinically. The validated model was then used to evaluate the effect of both superior translation of the humeral head and tension on the long head of the biceps tendon on the strain in the intact labrum. The humeral head motion was found to have relatively greater effect than the biceps tension on the initiation of the SLAP tear. Repetitive micro-trauma or tissue fatigue rather than a single loading event is most likely to cause a mid-substance failure of the labrum. This work also tested the effect of the biceps tension

on the propagation of SLAP tears using the finite element model. With loading of the biceps, the model predicted high strains at the edges of the tear suggesting a high risk for progression of the tear. For larger tears, the effect of the biceps was more pronounced. Based on this work, tear size is suggested as one criterion for determining the optimal treatment of the SLAP lesion. During development of the finite element model, simplifying assumptions were necessary. With careful consideration of the effect of these assumptions and simplifications on the results, the current work suggests a plausible mechanism of injury for SLAP lesions. This work is to identify the role of humeral head translation and biceps loading in the initiation and propagation of SLAP tears by examination of the predicted strain.

CHAPTER I

INTRODUCTION

Introduction

The shoulder, the most mobile joint in the human body, is made up of three bones: the humerus (upper arm bone), the scapula (shoulder blade), and the clavicle (collarbone). Among these bones, the head of humerus and the glenoid (the end of the scapula) form the glenohumeral joint. The current work focuses on the glenoid labrum tissue in the glenohumeral joint.

Anatomy of the Glenoid Labrum

The glenoid labrum is a ring of fibro-cartilaginous tissue in the glenohumeral joint (Figure 1.1). The glenohumeral joint is described as a golf ball-and-tee due to the large difference in the curvature and size between the head of the humerus and the glenoid. The labrum attaches to the glenoid rim and surrounds both glenoid cartilage and bone (Figure 1.2). The glenoid labrum has a triangular- or wedge-shaped cross section. The labrum also provides a site of attachment for the long head of the biceps tendon, and glenohumeral ligaments (Figure 1.3).[1] Specifically, the superior labrum serves as the anchor of the long head of the biceps tendon.

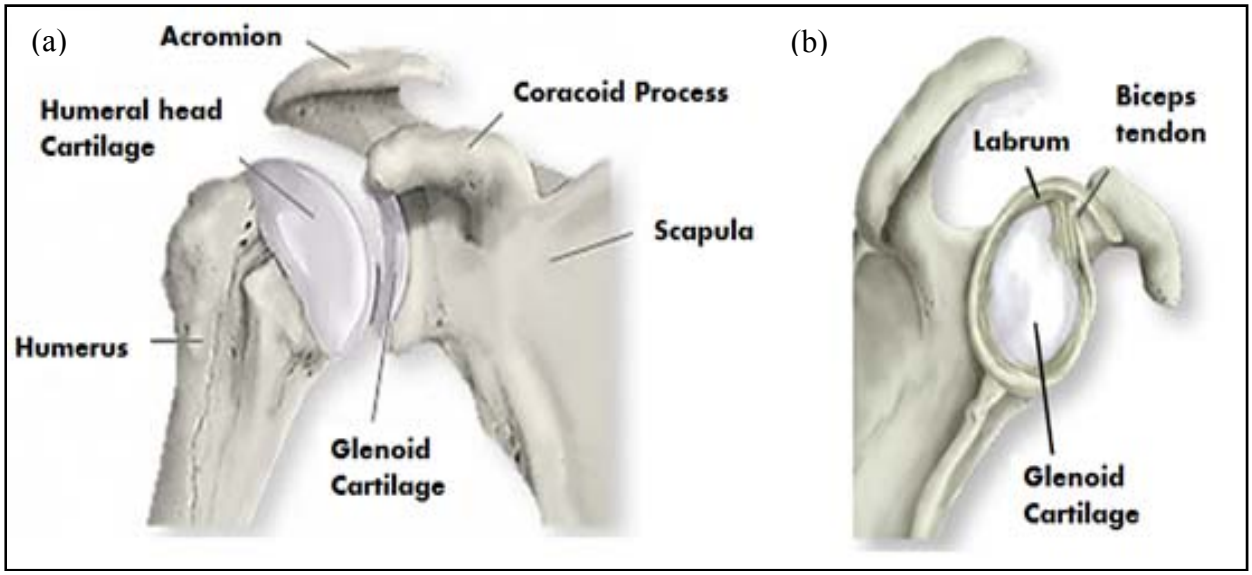

Figure 1.1 - The glenohumeral joint without muscles and capsules (a) in coronal view, and (b) in lateral view with the hidden humerus.[2]

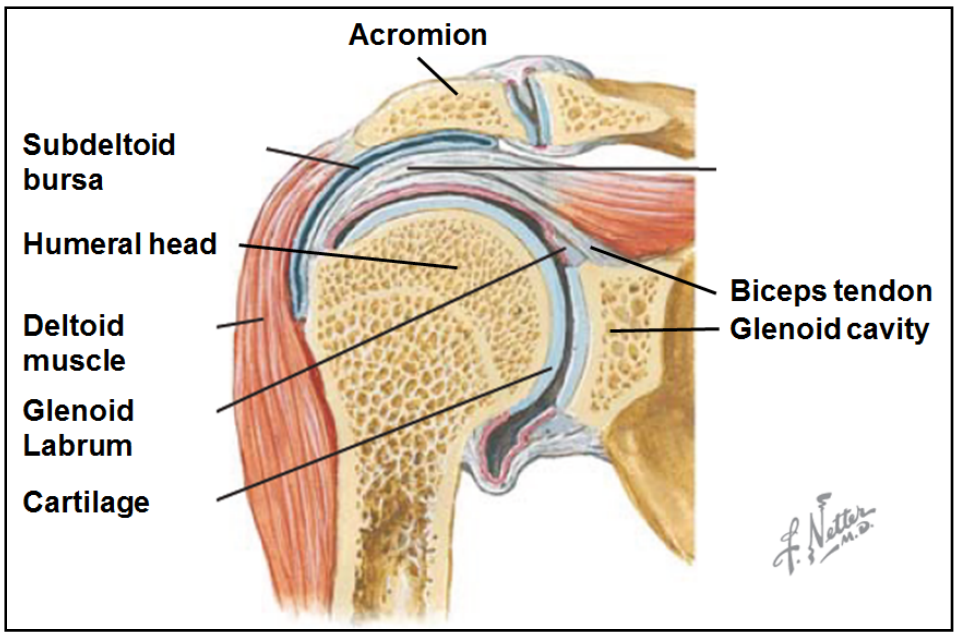

Figure 1.2 - The glenohumeral joint in coronal sectional view

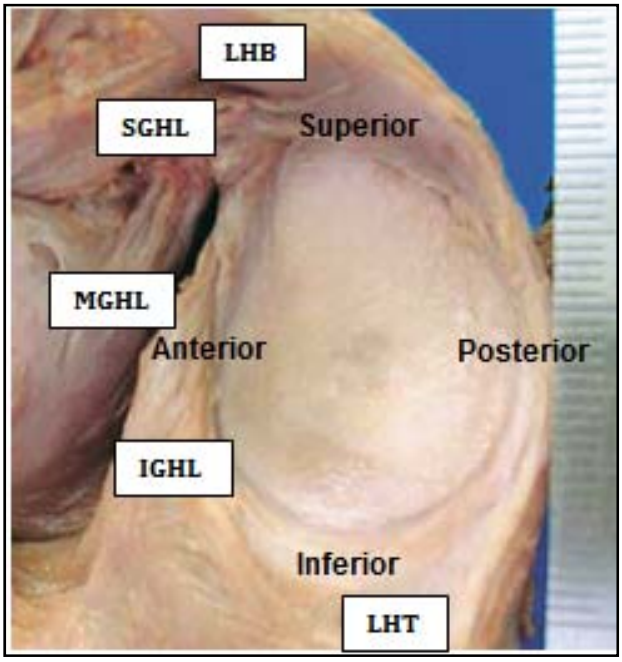

Figure 1.3 - The glenoid labrum with connective tissues except the posterior capsule in lateral view[3]. LHB, long head of the biceps tendon; SGHL, superior glenohumeral ligament; MGHL, medial glenohumeral ligament; IGHL, inferior glenohumeral ligament; LHT, long head of the triceps.

Function of the Glenoid labrum

The glenoid labrum increases the stability of the glenohumeral joint by increasing congruency between the glenoid and humeral head and by serving as the attachment for the connective tissues surrounding the articular joint. The balancing of the large, spherical humeral head on a much smaller, relatively flat glenoid does not produce a stable shoulder. Consequently, there is a need for substantial additional support of the soft tissues. The rotator cuff muscles and the superficial muscles are the active stabilizers for the glenohumeral joint, while the capsule, ligament, and the glenoid labrum are the passive stabilizers. The glenoid labrum contributes to the depth of the glenoid fossa by 30% to 50% [4,5] and extends the contact surface area.[6,7] Thus the labrum increases stability by 10% to 20%.[4,8] The glenoid labrum also forms a periarticular band of ligamentous and tendinous tissue by serving as the insertion site for connective tissues.[1,3] This mechanism is hypothesized as a tension brace against the humeral head translation[9] and a passive stabilizer.[10] In particular, the superior glenoid labrum is an anchoring point for the long head of the biceps tendon, which is a stabilizer of the humeral head on the glenoid during abduction.[11] The importance of the superior labrum-biceps complex in the stability and kinematics of the shoulders has been confirmed experimentally.[12,13,14,15]

Pathology of the Glenoid Labrum

Most problems in the glenoid labrum are found in association with problems in other tissues in the glenohumeral joint. When the anteroinferior labrum is detached from the glenoid rim, the inferior glenohumeral ligament on the labrum is also detached, termed a 'Bankart lesion'.[16] This Bankart lesion has been observed commonly with an anterior dislocation.[17] The tear between the posteroinferior labrum-ligament complex and the glenoid cartilage has been reported accompanying a multi or posterior shoulder instability.[18,19] The lesion of the superior labrum occurs both in the anterior and the posterior regions of the biceps anchor on the superior labrum.[20,21] This tear is often associated with dislocations,[12] and/or rotator cuff tears.[20,22]

Tear on the Superior Glenoid Labrum

With advanced clinical imaging techniques, pathologies of the glenoid labrum have been detected and the injury mechanisms have been actively theorized for the last three decades. Tears of the anterosuperior labrum from the glenoid were initially described by Andrews et al.[21] Later, Snyder et al. termed this tear a SLAP tear to represent lesions of the superior labrum from anterior to posterior.[20] SLAP tears are classified according to four or more types. [20,22,23] Although the reported incidence of each SLAP tear varies considerably depending on the literature,[24,25] there is a general agreement that the detachment of the superior labrum and biceps tendon from the underlying glenoid (Type II SLAP) is the most common symptomatic lesion of the superior labrum.[9,20]

Although multiple hypotheses for the mechanism of injury have been proposed, the mechanism for the tear is not clearly understood. The large biceps tension results from the repeated throwing motion was suspected to be the primary cause of the SLAP tear.[21] Grauer et al.[26] suggested that both the humeral head compression and biceps tendon traction were implicated in the SLAP tear. In contrast, Snyder et al. [27] postulated that the combination of a compression force and subluxation force on the humeral head from the rotator cuff may cause SLAP tears. The 'peel-back' mechanism, that results in torsional force to the biceps tendon, has also been suggested as a possible cause of SLAP tears.[28] In summary, both the translation of the humeral head and traction on the biceps tendon have been considered as the main factors in the causation of SLAP tears.

Approaches to Studying Superior Glenoid Labrum Tears

Diverse traditional methods in the clinical fields have been used to test theories for the pathology of the superior glenoid labrum, and more recently interdisciplinary approaches have been introduced. The ideal approach would be to examine the behavior of the labrum thorough out the tissue during specific motions, and at specific joint positions *in vivo*. However, none of current techniques are ideal since each method has its own limitation. For example, the histologic examinations[3,29,30] and the arthroscopic assessments[3,24,27,30,31] of the glenoid labrum are useful to get insight into the structure and anatomical variations of the labrum. However, these techniques can explain neither the function of the labrum, nor the tear mechanism of the glenoid labrum directly. With the biomechanical studies of the material characteristics of the labrum itself,[9,32,33] of the labrum-biceps complex,[34,35] or of the labrum after clinical treatment,[36,37] the weaknesses in the glenoid labrum and the general mechanical behavior of the intact, or repaired labrum can be tested. The biomechanical observations of the labral behavior during certain motions[38,39,40], or under specific condition [4,15,41] can also give insight into the role of the labrum and the risk for tears. The studies using cadavers limit the number of tests with the same specimen and allow only surface observations of the tissue. For these reasons, computational modeling has been suggested, [42,43,44] similar to other complex studies related to tissue mechanics.[45,46,47,48,49,50,51,52,53,54,55,56,57,58] The most significant challenge to the computational approach is the need to determine the reliability of predictions by appropriate validation process.

Chapter Overviews

This thesis proposes that **the strain distribution predicted by a finite element model explains the mechanical behavior of the superior glenoid labrum**. The validated finite element model for the glenohumeral joint including the humerus, glenoid, articular cartilages, labrum, and the biceps tendon predicts the strain pattern. Based on a demonstrated strong relationship between strain distribution in the tissue and tear propagation,[59] how a factor contributes to the predicted stain distribution explains the impact of each factor on the development of tears in the superior labrum.

The purpose of Chapter I is to present the current state of knowledge concerning the superior glenoid labrum. Chapter II is then validates a finite element model for the mechanism of tears in the superior glenoid labrum. Chapter III focuses on determining the risk of injury to the superior glenoid labrum due to the superior translation of the humeral head, as can be seen in cases of rotator cuff tears, combined with tensile loading on the long head of the biceps tendon. Chapter IV investigates the effect of tension on the long head of the biceps tendon on the propagation of the SLAP tear by observing the mechanical behavior of the torn superior glenoid labrum. Chapter V discusses the findings, strength, limitations, and future direction of this study. Finally, chapter VI provides a summary of the behavior of the superior glenoid labrum.

To fulfill each purpose, multiple hypotheses are suggested and tested. The following working hypotheses will be tested.

Hypothesis in Chapter II:

Superior translation of the humeral head and tension on the long head of the bicep tendon cause a displacement of the superior labrum relative to the glenoid and a concomitant increase in tissue strain.

Hypotheses in Chapter III:

(1) The regions of high strain in the labrum occur along a crescent in the mid-substance of the superior labrum corresponding to common superior labral lesions (types I and II)

(2) Increasing load on the long head of the biceps tendon causes increased strain in the labrum.

(3) The effect of superior humeral head translation on the increasing strain in the labrum is greater than the effect of biceps tension.

Hypotheses in Chapter IV:

(1) The regions of high strain in the torn labrum occur at the edge of the given tear.

(2) Increasing load on the long head of the biceps tendon causes increased strain in the torn labrum regardless of the tear size.

(3) The effect of the biceps tension on the increasing strain in the torn labrum is greater than that in the intact labrum.

References

1. Huber, W.P., Putz, R.V., 1997. Periarticular fiber system of the shoulder joint. Arthroscopy 13, 680-691.

2. Southern California Orthopedic Institute (SCOI), Shoulder: Anatomy of the Shoulder. Available at: http://www.scoi.com/shoulder.php Accessed 13 Dec 2013.

3. Tuoheti, Y., Itoi, E., Minagawa, H., Yamamoto, N., Saito, H., Seki, N., Okada, K., Shimada, Y., Abe, H., 2005. Attachment types of the long head of the biceps tendon to the glenoid labrum and their relationships with the glenohumeral ligaments. Arthroscopy 21, 1242-1249.

4. Lippitt, S., Matsen, F., 1993. Mechanisms of glenohumeral joint stability. Clinical Orthopaedics and Related Research 291, 10-28.

5. Howell, S.M., Galinat, B.J., 1989. The glenoid-labral socket. Clinical Orthopaedics and Related Research 243, 122-125.

6. Greis, P.E., Scuderi, M.G., Mohr, A., Bachus, K.N., Burks, R.T., 2002. Glenohumeral articular contact areas and pressures following labral and osseous injury to the anteroinferior quadrant of the glenoid. Journal of Shoulder and Elbow Surgery 11, 442-451.

7. Bey, M., 2001. Injury mechanism of the shoulder: quantitative analysis of tendons and ligaments. University of Michigan

8. Fehringer, E.V., Schmidt, G.R., Boorman, R.S., Churchill, S., Smith, K.L., Norman, A.G., Sidles, J.A., Matsen III, F.A., 2003. The anteroinferior labrum helps center the humeral head on the glenoid. Journal of Shoulder and Elbow Surgery 12, 53-58.

9. Smith, C.D., Masouros, S.D., Hill, A.M., Wallace, A.L., Amis, A.A., Bull, A.M., 2009. The compressive behavior of the human glenoid labrum may explain the common patterns of SLAP lesions. Arthroscopy 25, 504-509.

10. McMahon, P.J., Burkart, A., Musahl, V., Debski, R.E., 2004. Glenohumeral translations are increased after a type II superior labrum anterior-posterior lesion: a cadaveric study of severity of passive stabilizer injury. Journal of Shoulder and Elbow Surgery 13, 39-44.

11. Warner, J.J.P., McMahon, P.K., 1995. The role of the long head of the biceps brachii in superior stability of the glenohumeral joint. Journal of Bone and Joint Surgery (American) 77-A, 366-372.

12. Pagnani, M.J., Speer, K.P., Altchek, D.W., Warren, R.F., Dines, D.M., 1995. Arthroscopic fixation of superior labral lesions using a biodegradable implant: a preliminary report. Arthroscopy 11, 194-198.

13. Burkhart, A., Debski, R.E., Musahl, V., McMahon, P.J., Woo, S.L., 2003.

Biomechanical tests for type II SLAP lesions of the shoulder joint before and after arthroscopic repair. Orthopade 32, 600-607

14. Panossian, V., Mihata, T., Tibone, J.E., Fitzpatrick, M.J., McGarry, M.H., Lee, T.Q., 2005. Biomechanical analysis of isolated type II SLAP lesions and repair. Journal of Shoulder and Elbow Surgery 14, 529-534.

15. Patzer, T., Habermeyer, P., Hurschler, C., Bobrowitsch, E., Wellmann, M., Kircher, J., Schofer, M.D., 2010. The influence of superior labrum anterior to posterior (SLAP) repair on restoring baseline glenohumeral translation and increased biceps loading after stimulated SLAP tear and the effectiveness of SLAP repair after long head of biceps tenotomy. Journal of Shoulder and Elbow Surgery 21, 1580-1587.

16. Bankart, A.S.B., 1923. Recurrent or habitual dislocation of the shoulder-joint. The British Medical Journal, 1132-1133.

17. Antonio, G.E., Griffith, J.F., Yu, A.B., Yung, P.S.H., Chan, K.M., Ahuja, A.T., 2007. First-time shoulder dislocation: high prevalence of labral injury and age-related differences revealed by MR arthrography. Journal of Magnetic Resonance Imaging 26, 983-991.

18. Yu, J.S., Ashman, C.J., Jones, G., 2002. The POLPSA lesion: MR imaging findings with arthroscopic correlation in patients with posterior instability. Skeletal Radiology 31, 396-399.

19. Kim, S., Ha, K., Yoo, J., Noh, K., 2004. Kim's lesion: an incomplete and concealed avulsion of the posteroinferior labrum in posterior or multidirectional posteroinferior instability of the shoulder. Arthroscopy 20, 712-720.

20. Snyder, S.J., Karzel, R.P., Pizzo, W.D., Ferkel, R.D., Friedman, M.J., 1990. SLAP lesions of the shoulder. Arthroscopy 6, 274-279.

21. Andrews, J.R., Carson, W.G., Mcleod, W.D., 1985. Glenoid labrum tears related to the long head of the biceps. American Journal of Sports Medicine 13, 337-341.

22. Morgan, C.D., Burkhart, S.S., Palmeri, M., Gillespie, M., 1998. Type II SLAP lesions: three subtypes and their relationships to superior instability and rotator cuff tears. Arthroscopy 14, 553-565.

23. Maffet, M.W., Gartsman, G.M., Moseley, B., 1995. Superior labrum-biceps tendon complex lesions of the shoulder. American Journal of Sports Medicine 23, 93-98.

24. Kim, T.K., Queale, W.S., Cosgarea, A.J., McFarland, E.G., 2003. Clinical features of the different types of SLAP lesions: an analysis of one hundred and thirty-nine cases. Journal of Bone and Joint Surgery (American) 85-A, 66-71.

25. Werner, C.M.L., Nyffeler, R.W., Jacob, H.A.C., Gerber, C., 2004. The effect of capsular tightening on humeral head translations. Journal of Orthopaedic Research 22, 194-201.

26. Grauer, J.D., Paulos, L.E., Smutz, W.P., 1992. Biceps tendon and superior labral injuries. Arthroscopy 8, 488-497.

27. Snyder, S.J., Banas, M.P., Karzel, R.P., 1995. An analysis of 140 injuries to the superior glenoid labrum. Journal of Shoulder and Elbow Surgery 4, 243-248.

28. Burkhart, S.S., Morgan, C.D., 1998. The peel-back mechanism: its role in producing and extending posterior type II SLAP lesions and its effect on SLAP repair rehabilitation. Arthroscopy 14, 637-640.

29. Hill, A.M., Hoerning E.J., Brook, K., Smith, C.D., Moss, J., Ryder, T., Wallace, A.L., Bull, A.M.J., 2008. Collagenous microstructure of the glenoid labrum and biceps anchor. Journal of Anatomy 212, 853-862.

30. Pfahler, M., Haraida, S., Schulz, C., Anetzberger, H., Refior, H.J., Bauer, G.S., Bigliani, L.U., 2003. Age-related changes of the glenoid labrum in normal shoulders. Journal of Shoulder and Elbow Surgery 12, 40-52.

31. Vangsness, C.T., Jr., Jorgenson, S.S., Watson, T., Johnson, D.L., 1994. The origin of the long head of the biceps from the scapula and glenoid labrum. An anatomical study of 100 shoulders. Journal of Bone and Joint Surgery (British) 76, 951-954.

32. Carey, J., Small, C.F., Pichora, D.R., 2000. In situ compressive properties of the glenoid labrum. Journal of Biomedical Materials Research 51, 711-716.

33. Smith, C.D., Masouros, S.D., Hill, A.M., Wallace, A.L., Amis, A.A., Bull, A.M., 2008. Tensile properties of the human glenoid labrum. Journal of Anatomy 212, 49-54.

34. Costa Ado, S., Leite, J.A., Melo, F.E., Guimaraes, S.B., 2006. Biomechanical properties of the biceps-labral complex submitted to mechanical stress. Acta Cirurgica Brasileira 21, 214-218.

35. Bey, M.J., Elders, G.J., Huston, L.J., Kuhn, J.E., Blasier, R.B., Soslowsky, L.J., 1998. The mechanism of creation of superior labrum, anterior, and posterior lesions in a dynamic biomechanical model of the shoulder: the role of inferior subluxation. Journal of Shoulder and Elbow Surgery 7, 397-401.

36. DiRaimondo, C.A., Alexander, J.W., Noble, P.C., Lowe, W.P., Lintner, D.M., 2004. A biomechanical comparison of repair techniques for type II SLAP lesions. American Journal of Sports Medicine 32, 727-733.

37. Uggen, C., Wei, A., Glousman, R.E., ElAttrache, N., Tibone, J.E., McGarry, M.H., Lee, T.Q., 2009. Biomechanical comparison of knotless anchor repair versus simple suture repair for type II SLAP lesions. Arthroscopy 25, 1085-1092.

38. Pradhan, R.L., Itoi, E., Hatakeyama, Y, Urayama, M., Sato, K., 2001. Superior labral strain during the throwing motion: a cadaveric study. American Journal of Sports Medicine 29, 488-492.

39. Rizio, L., Garcia, J., Renard, R., Got, C., 2007. Anterior instability increases superior labral strain in the late cocking phase of throwing. Orthopedics 30, 544-550.

40. Kuhn, J.E., Lindholm, S.R., Huston, L.J., Soslowsky, L.J., Blasier, R.B., 2003. Failure of the biceps superior labral complex: a cadaveric biomechanical investigation comparing the late cocking and early deceleration positions of throwing. Arthroscopy 19, 373-379.

41. Healey, J.H., Barton, S., Noble, P., Kohl, H.W., 3rd, Ilahi, O.A., 2001. Biomechanical evaluation of the origin of the long head of the biceps tendon. Arthroscopy 17, 378-382.

42. Yeh, M.L., Lintner, D., Luo, Z.P., 2005. Stress distribution in the superior labrum during throwing motion. American Journal of Sports Medicine 33, 395-401.

43. Gatti, C.J., Maratt, J.D., Palmer, M.L., Hughes, R.E., Carpenter, J.E., 2010. Development and validation of a finite element model of the superior glenoid labrum. Annals of Biomedical Engineering 38, 3766-3776.

44. Drury, N.J., Ellis, B.J., Weiss, J.A., McMahon, P.J., Debski, R.E., 2010. The impact of glenoid labrum thickness and modulus on labrum and glenohumeral capsule function. Journal of Biomechanical Engineering 132, 121003.

45. Oomens, C.W.J., Bressers, O.F.J.T., Bosboom, E.M.H., Bouten, C.V.C., Bader, D.L., 2003. Can loaded interface characteristics influence strain distributions in muscle adjacent to bony prominences? Computer Methods in Biomechanics and Biomedical Engineering 6, 171-180.

46. Wakabayashi, I., Itoi, E., Sano, H., Shibuya, Y., Sashi, R., Minagawa, H., Kobayashi, M., 2003. Mechanical environment of the supraspinatus tendon: a two-dimensional finite element model analysis. Journal of Shoulder and Elbow Surgery 12, 612-617.

47. Anderson, A.E., Peters, C.L., Tuttle, B.D., Weiss, J.A., 2005. Subject-specific finite element model of the pelvis: development, validation and sensitivity studies. Journal of Biomechanical Engineering 127, 364-373

48. Blemker, S.S., Pinsky, P.M., Delp, S.L., 2005. A 3D model of muscle reveals the causes of nonuniform stains in the biceps brachii. Journal of Biomechanics 38, 657-665.

49. Yao, J., Snibbe, J., Maloney, M., Lerner, A.L., 2006. Stresses and strains in the medial meniscus of an ACL deficient knee under anterior loading: a finite element analysis with image-based experimental validation. Journal of Biomechanical Engineering 128, 135-141.

50. Ellis, B.J., Debski, R.E., Moore, S.M., McMahon, P.J., Weiss, J.A., 2007. Methodology and sensitivity studies for finite element modeling of the inferior glenohumeral ligament complex. Journal of Biomechanics 40, 603–612

51. Anderson, A.E., Ellis, B.J., Maas, S.A., Peters, C.L., Weiss, J.A., 2008, Validation of finite element predictions of cartilage contact pressure in the human hip joint. Journal of Biomechanical Engineering 130, 051008

52. Anderson, A.E., Ellis, B., Maas, S., Weiss, J.A., 2010. Effects of idealized joint geometry on finite element predictions of cartilage contact stresses in the hip. Journal of Biomechanics 43, 1351-1357.

53. Drury, M.J., Ellis, B.J., Weiss, J.A., McMahon, P.J., Debski, R.E., 2011. Finding consistent strain distributions in the glenohumeral capsule between two subjects: implications for development of physical examinations. Journal of Biomechanics 44, 607-613.

54. Elkins, J.M., Stroud, N.J., Rudert, M. J., Tochigi, Y., Pedersen, D.R., Ellis, B.J., Callaghan, J.J., Weiss, J.A., 2011. The capsule's contribution to total hip constructs stability – a finite element analysis. Journal of Orthopaedic Research 29, 1642-1648.

55. Harris, M.D., Anderson, A.E., Henak, C.R., Ellis, B.J., Peters, C.L., Weiss, J.A., 2012. Finite element prediction of cartilage contact stresses in normal human hips. Journal of Orthopaedic Research 30, 1133-1139.

56. Henak, C.A., Ellis, B.J., Harris, M.D., Anderson, A.E., Peters, C.L., Weiss, J.A., 2011. Role of the acetabular labrum in load support across the hip joint. Journal of Biomechanics 44, 2201-2206.

57. Inoue, A., Chosa, E., Goto, K., Tajima, N., 2012. Nonlinear stress analysis of the supraspinatus tendon using three-dimensional finite element analysis. Knee Surgery, Sports Traumatology, Arthroscopy 21, 1151-1157.

58. Smith, M.V., Panchal, H.B., Ruberte, R.A., Thiele, R., Sekiya, J. K., 2012. Effect of acetabular labrum tears on hip stability and labral strain in a joint compression model. American Journal of Sports Medicine 39, 103S.

59. Andarawis-Puri, N., Ricchetti, E.T., Soslowsky, L.J., 2009. Rotator cuff tendon strain correlates with tear propagation. Journal of Bioemechanics 42, 158-163.

CHAPTER II

VALIDATE A FINITE ELEMENT MODEL FOR THE PATHOLOGY OF THE SUPERIOR GLENOID LABRUM

(Accepted by Journal of Biomechanics)

Introduction

More than 4.1 million patients present annually with symptoms related to the rotator cuff of the shoulder. After the third and fifth decades of life, approximately 30% and 80%, respectively, of patients will have rotator cuff tears,[1] the most common injury to shoulder joints. Tears are frequently accompanied by an associated injury to the superior glenoid labrum.[2] Tears of the superior glenoid labrum are believed to cause pain and mechanical symptoms of catching and locking in the shoulder. Treatments include debridement and/or repair of the labrum and release and tenodesis of the biceps tendon.

Mechanically, the glenohumeral joint is capable of the largest range of motion in the human body. The large difference between the curvature and size of the humeral head compared with the glenoid requires both active stabilization by the rotator cuff muscles and passive stabilization by the concavity of the glenoid. The variation in cartilage thickness improves

congruency between the two bones[3] as does the fibrocartilaginous labrum, which increases the surface area and glenoid depth.[4,5] Similar to the meniscus of the knee and the labrum of the hip, the strain experienced by the labrum correlates with susceptibility to injury. However, *in situ* measurements of strain in the glenoid labrum remain difficult due to the small size of the tissue and its location between the glenoid cartilage, glenoid bone, and the humeral head. The role of both active and passive factors in stabilizing the glenohumeral joint, and observations that rotator cuff tears are associated with increased superior humeral head translation,[6,7,8] suggest that a causal relationship may exist between rotator cuff pathology and increased strain in the superior labrum.

In addition to its role as a passive stabilizer of the glenohumeral joint, the superior labrum is also contiguous with the origin of the long head of the biceps tendon.[9,10,11] Increased biceps tension in activities like overhead throwing may alter glenohumeral kinematics[12] and increase strain on the labrum.[13,14]

The effects of superior humeral head migration and biceps tension on labral strain are not well established. Moreover, the effect of the constitutive model on the predicted mechanics of the labrum is not well understood. Previous studies that analyzed the distribution of stress and strain in the labrum used a linear, isotropic constitutive law and modeled the morphology of the labrum as a thin two-dimensional shell structure[15] or derived the three-dimensional morphology from regular geometric shapes.[13] The previous Gatti's work[16] demonstrated the efficacy of the finite element model in predicting the displacements and strain in the labrum during humeral head translation using a linear, transversely isotropic hyperelastic constitutive law. The present study extends this work by coupling nonlinear constitutive models of the labrum with a subject-specific model of the morphology of the labrum, including the interface with and tension on the

biceps tendon. The purpose was to analyze the interaction of labrum mechanics and cuff dysfunction by (i) validating an extended finite element model with primary experimental data that includes the effects of biceps loading, (ii) determining the effect of the constitutive model on the predicted labral response, and (iii) predicting the strain distribution within the superior labrum. We hypothesize that superior humeral head translation, as can be seen in rotator cuff disease, and biceps tension may play a role in the development of labral pathology in patients with rotator cuff tears. The hypothesis will be supported if superior translation of the humeral head and tension on the long head of the biceps tendon causes a displacement of the superior labrum relative to the glenoid and a concomitant increase in tissue strain.

Methods

A right shoulder with no signs of previous injury was obtained from a fresh-frozen cadaver (male, 84 years old) and dissected free of all soft tissue, except for the labrum, the origin of the biceps tendon, and the cartilages on both the glenoid and humeral head. The specimen was then scanned using a micro-CT system (GE eXplore Locus, GE Healthcare–Pre-Clinical Imaging, London, UK). Because the soft tissues were difficult to distinguish in the micro-CT images, the labrum and biceps tendon origin were then removed and the specimen was rescanned. A Boolean operation was then applied to the two image sets allowing segmentation and 3D reconstruction of the humeral head bone, humeral head cartilage, glenoid bone, glenoid cartilage, labrum, and the biceps origin using Amira (Visage Imaging, Inc., San Diego, CA).

The segmented structures were converted to surface entities and smoothed before exporting them to Hypermesh (Altair Engineering, Inc., Troy, MI), a finite element pre-processing tool. The bones were modeled using quadrilateral shell elements.[17] The cartilages, labrum, and biceps origin were converted to hexahedral solid elements.[16,18,19] To simulate the clinically precise biceps tensile vector, hexahedral elements were added to the distal end of the biceps tendon by following the biceps groove. The labrum was sectioned into superior, anterior, inferior, and posterior labrum. Each of the labral sections and the biceps tendon were assigned local coordinate systems to define the local fiber orientation.[16] A mesh convergence study for the glenoid, glenoid cartilage, labrum, and biceps tendon was performed adjusting the mesh density to ensure the numerical stability of the result. The resulting finite element mesh contained 6071 solid elements, 9331 shell elements, and 16261 nodes (Figure 2.1). Doubling the mesh density produced a strain difference of approximately 1% and a displacement difference of less than 1%, but caused a 10-fold increase in solution time.

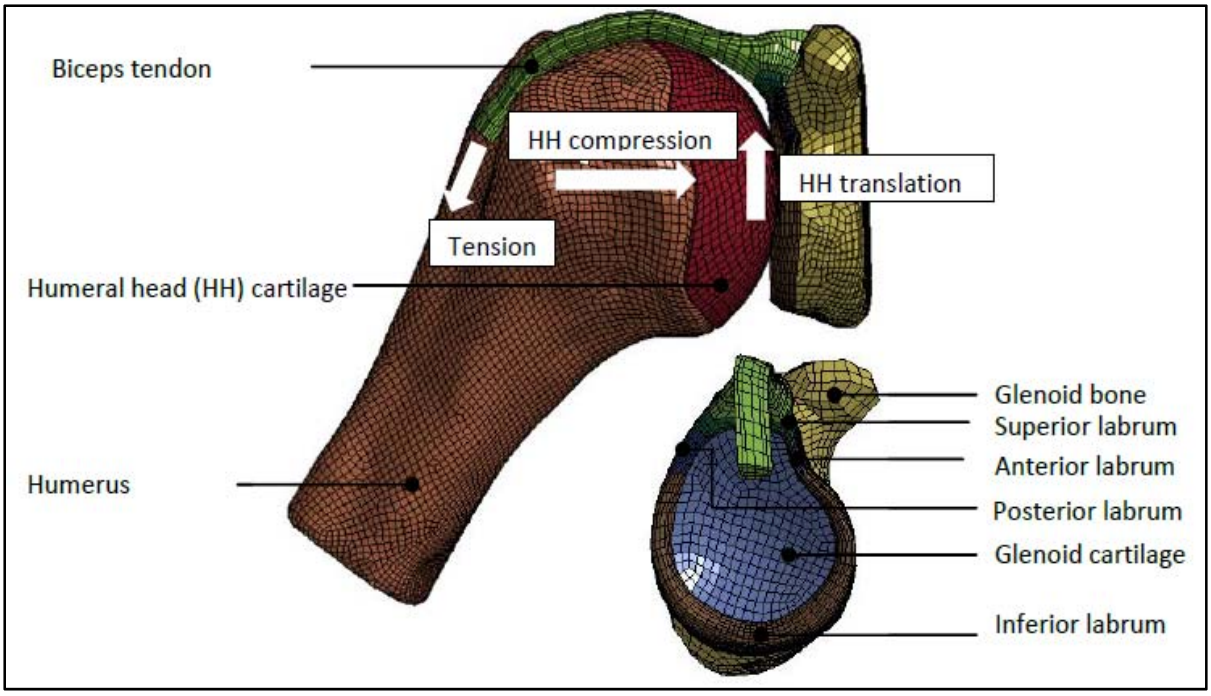

Figure 2.1 - Three-dimensional finite element model of the glenohumeral joint, including the labrum-biceps complex. The humerus is shown in coronal view and was hidden in lateral view.

Baseline material properties for each tissue were assigned based on the literature (Table 1). The bones were modeled as rigid materials because of their relatively small deformations compared to other soft tissues and the modest loading conditions in our model.[17] The cartilages were modeled as isotropic elastic materials.[16,20] The labrum was modeled as a transversely isotropic material,[21] since there is a difference of approximately two orders of magnitude between the modulus in the transverse plane and the circumferential direction.[22] The labrum material coefficients for the hyperelastic model were obtained by fitting the neo-Hookean constitutive equation to an experimentally derived expression for uniaxial hyperelastic behavior along the fiber direction.[19,23] Similarly, the biceps tendon was modeled as a transversely isotropic, hyperelastic material with an elastic modulus of 629 MPA.[24] This modulus was chosen because it was obtained from a shoulder without rotator cuff tears at a location closer to the labrum than in other studies.[25]

Table 2.1 - Baseline material properties of the components in a three dimensional model of the glenohumeral joint

Anatomy	Material Type	Parameter	Value	References
Humerus	Rigid	E	12 GPa	26
Humeral Cartilage	Isotropic elastic	E	0.66 MPa	17, 20
		ρ	1075 kg/m^3	16
		υ	0.08	17
Labrum	Transversely isotropic, hyperelastic	ρ	1225 kg/m^3	16
		C1	1.142 MPa	22
		C3	0.05 MPa	22
		C4	36	22
		C5	60.5 MPa	22
		λ*	1.138	22
Biceps tendon	Isotropic hyperelastic	ρ	1225 kg/ m^3	16
		C1	0.138 MPa	24
		C3	0.002 MPa	24
		C4	0.061 MPa	24
		C5	0.641 MPa	24
		λ*	1.100	24
Glenoid Cartilage	Isotropic elastic	E	1.7 MPa	16, 27
		ρ	1075 kg/m^3	16
		υ	0.018	16
Glenoid	Rigid	E	100 MPa	28

Boundary conditions for the finite element model were chosen to simulate the experimental conditions. The basic experimental protocol was published previously[16] and was extended to include biceps loading (Figure 2.2). We positioned the humerus in 30˚ of glenohumeral abduction in the scapular plane with neutral humeral rotation. A compressive force of 50 N in the medial direction was applied to seat the humerus in the glenoid cavity.[4,16] Next, either 0 N or 22 N was applied to the distal end of the biceps tendon. A 22 N load was chosen because this load was shown to affect glenohumeral range of motion and kinematics.[12,16] Finally,

the humerus was translated in the superior direction relative to the glenoid between the starting position and a peak displacement. Peak displacement ranged 1-5 mm in increments of 1 mm. The superior direction was determined by drawing a line from the center of the glenoid to the biceps tendon attachment.[29] This range of displacements was used to validate the model across the spectrum of humeral head displacements that occur in healthy shoulders and ones with massive rotator cuff pathology.[7] The non-sliding interfaces were modeled using tied contact. All sliding interfaces were modeled using frictionless, surface-to-surface contact due to the low coefficient of friction in synovial joints.[19]

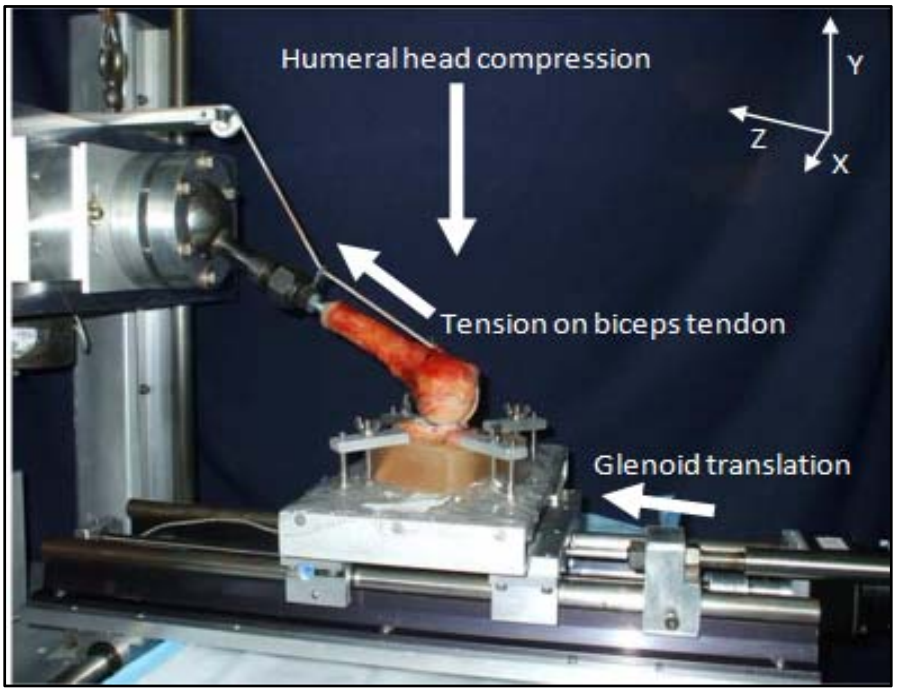

Figure 2.2 - Testing fixture for the validation experiment. Details of the basic experimental methods have been reported.[16] On top of this setting, 22 N of tensile loading was tested by attached to a 2.2 Kg weight at the end of the nylon rope.

The dynamic finite element analyses were performed using LS-DYNA Explicit (Livermore Software Technology Corp., Livermore, California). The predicted labral displacements were compared with data from a cadaver experiment. Since the experimental displacement was measured using plain radiographs parallel to the glenoid plane, the

displacement component in the out-of-glenoid plane was not used when determining the labrum displacement from the finite element analysis. The model also predicted the effective strain in the labrum as a function of the humeral head translation both with and without biceps tension. The effective von Mises strain was chosen because it is a scalar quantity representing the combined effect of all the components of the material strain tensor and indicative of the energy required to distort the material.[30] After averaging the effective strain for all elements within designated cross-sections through the labrum, we identified the average strain profile circumferentially along the superior labrum.

We also performed the material sensitivity test to assess the influence of the constitutive model and elastic moduli of both the labrum and articular cartilages on the prediction of the labral behavior.[31] The transversely isotropic hyperelastic constitutive model for the labrum was replaced with a transversely isotropic linearly elastic model.[22,32] Additionally, the effect of the labrum fiber stiffness was tested over a range of ±1 published standard deviation[22] using the hyperelastic model. The coefficients for the transversely isotropic, nonlinear hyperelastic constitutive law[23] used for the superior, anterior, inferior, and posterior labrum were calculated from 21.3 ± 9.4, 15.4 ± 5.0, 19.3 ± 5.9, and 20.9 ± 14.8 MPa of Young's modulus, respectively. Similarly, effects of the cartilage material law were tested by replacing the isotropic elastic model with a hyperelastic model and by varying the Young's modulus (0.66 ± 0.09 MPa, 1.7 ± 0.75 MPa) and Poisson's ratio (0.08 ± 0.06, 0.018 ± 0.026) over a range of ±1 standard deviation.[27,33,34]

The effect of the humeral head displacement, position along the labrum, and biceps tension on the labral displacements from the experimental protocol were assessed using repeated-measures 1-way ANOVAs. The effect of the constitutive model on the labral behavior was

assessed based on the predicted displacement and strain by finite element analysis. To validate the finite element model, we performed a linear regression analysis between predicted (finite element model) and observed (six experimental specimens) displacement of the labrum. The labral displacements were compared at each position along the labrum in each biceps tension condition with each humeral head displacement. All statistical analyses were performed using SPSS Version 20 (IBM Corp, Armonk, New York), with significance set at 0.05.

Results

Effect of humeral head displacement

Displacement of the labrum relative to the glenoid was significantly affected by superior translation of the humeral head ($P < 0.0002$) and position along the labrum ($P < 0.01$). The displacements predicted by the model with baseline material properties fell within 1 standard deviation of the labral displacements measured in the experiments (Figure 2.3). The predicted displacements were strongly correlated with the mean from the experiments at each position along the labrum for 0 N ($r = 0.68$, $P < 0.01$) and 22 N ($r = 0.84$, $P < 0.01$) of biceps tension. The highest displacements were observed at the biceps origin on the labrum. As the distance from the biceps origin along the labrum increased, the labral displacement also decreased. With increasing humeral head translation, labral displacement also increased.

Effect of tension on the long head of the biceps tendon

Tension on the biceps increased displacement of the labrum. With biceps loading, a shift was observed in the location of the maximum labral displacement from the anterior to the posterior labrum (Figure 2.3). The maximum mean and standard deviation of labral displacements in the loaded condition were 2.1 mm and 1.5 mm, while those values were 1.2 mm and 0.8 mm in the unloaded condition in the experimental data. With biceps tension, the predicted displacements differed from the mean of the experimental data by 0.1 mm and followed the same trend as the measured displacement profile along the labrum. The maximum difference between predicted and observed displacements occurred at the insertion of the biceps tendon on the labrum.

(a)

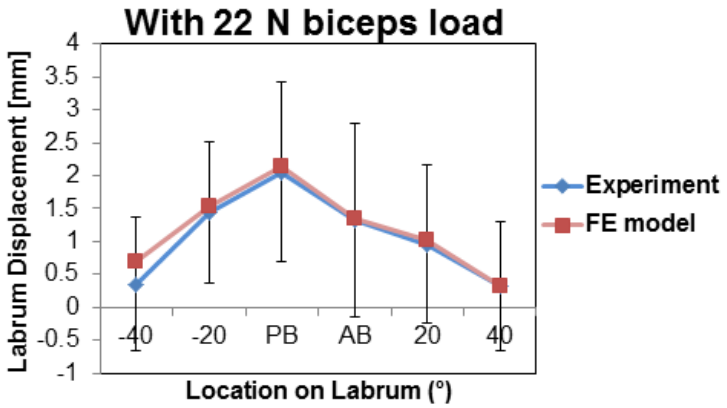

(b)

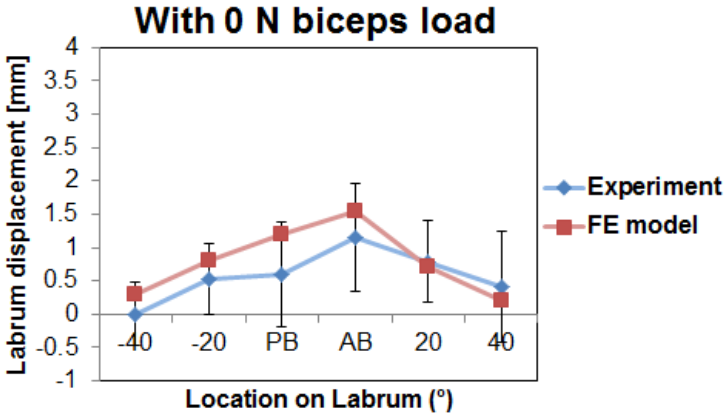

(c)

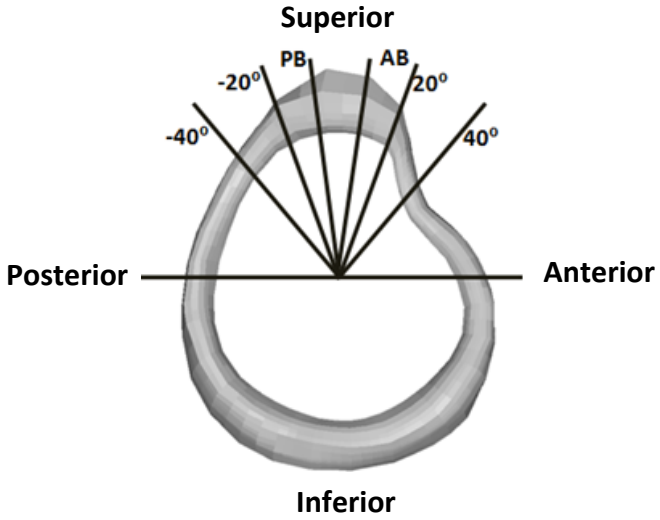

Figure 2.3 - Displacement profile of the superior labrum determined from the finite element model and experiments (average ± 1standard deviation) for 5mm of superior humeral head translation (a) with 22 N biceps load and (b) in the absence of biceps load on the long head of the biceps tendon at (c) different locations along the superior labrum. The labrum is shown in lateral view.

Effect of constitutive model

Compared with the elastic material law, the hyperelastic law for the labrum provided a smaller difference from the measured displacement (Figure 2.4a). Changing the labral constitutive law from hyperelastic to elastic increased the root mean square deviation between the mean experimental displacements and the predictions for the 22 N biceps tension (0.061 to 0.207 mm) and in the absence of biceps load (0.141 to 0.144 mm). Changes in the constitutive law for the labrum had a greater effect on the labral displacement and strain patterns than varying the material parameters for the labrum (Figure 2.4). Varying the modulus of the labrum by 1 standard deviation in the hyperelastic model resulted in a change of <0.1 mm in labral displacement and less than ±1% in strain. The constitutive laws and the parameters for the articular cartilages had minimal effect on both labral displacement and strain patterns. Altering the constitutive model and varying both the moduli and Poisson's ratio by 1 standard deviation of the values reported in the literature for the cartilages resulted in differences of <0.1 mm in displacement and <1% in strain.

Strain pattern

The finite element model predicted the region of highest strain in the superior labrum at the interface with the glenoid cartilage and glenoid bone along a crescent from approximately -20° (posterosuperior) to +40° (anterosuperior) with respect to the inferior-superior axis (Figure 2.4b). This high-strain region also extended through the labrum from the interface surface to the free surface in a radial direction (Figure 2.5a, inset). The peak average strain was located at 0° below the origin of the biceps tendon with a magnitude of 17%.

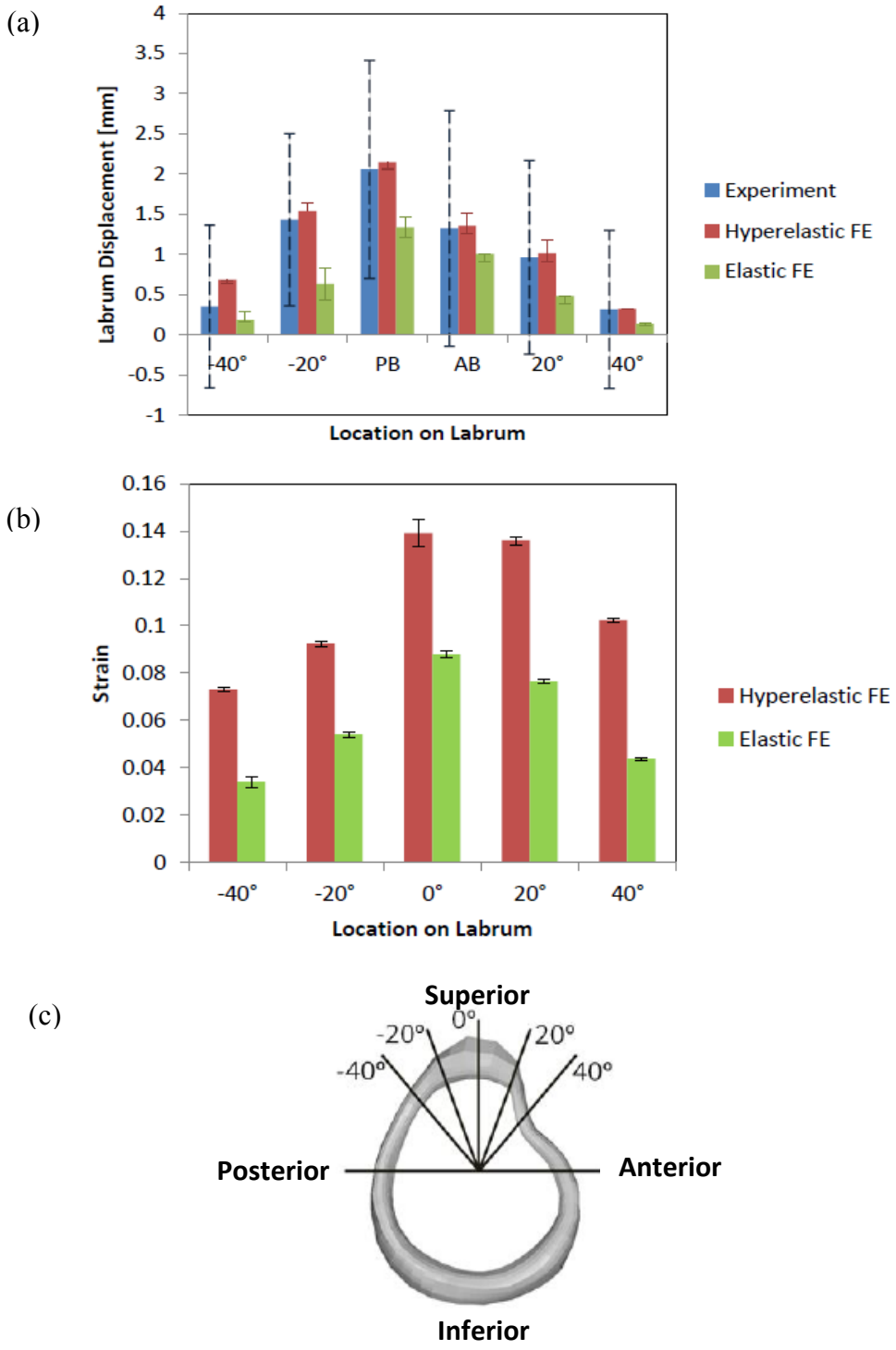

Figure 2.4 - The effect of variation in the labrum material parameters by ±1standard deviation on (a) the labral displacement and (b) the average strain through the cross section of the labrum due to 5mm of superior humeral head translation and 22 N of biceps loading at (c) specific locations along the superior labrum. The dashed line in (a) denotes the experimental standard deviation. The error bars (solid lines) in (a) and (b) were calculated from varying properties for the computational data. The labrum is shown in lateral view.

(a)

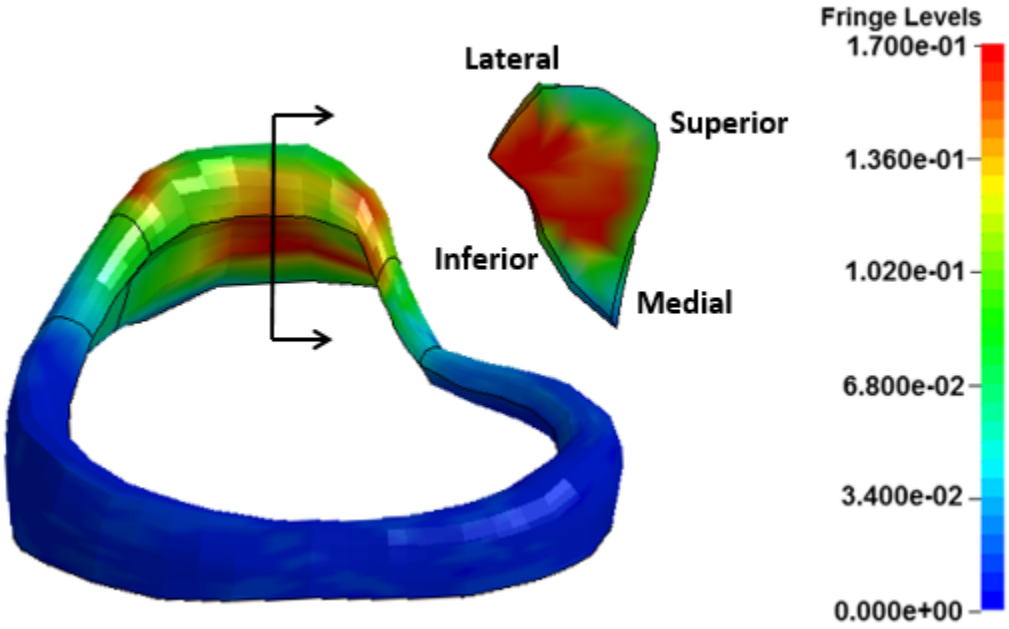

(b)

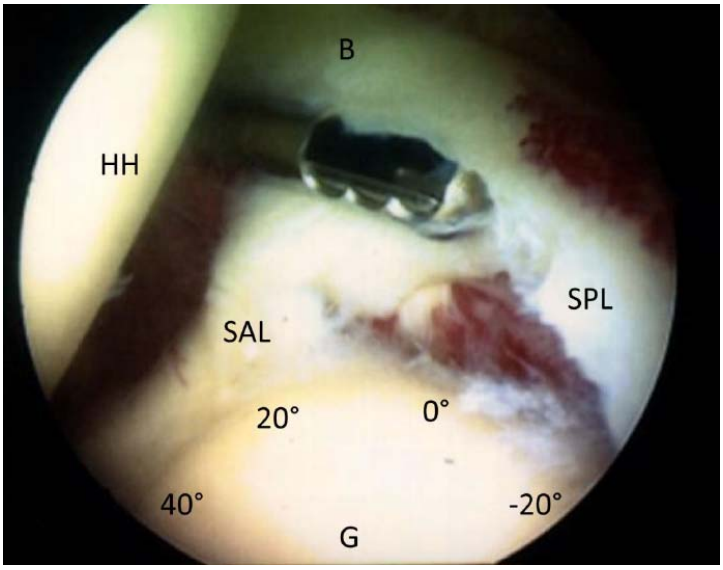

Figure 2.5 - Comparison between (a) the strain distribution predicted by the model with 22 N biceps tendon load and 5 mm of superior humeral head displacement and (b) a clinical observation of a superior labrum anterior posterior lesion. HH, humeral head; B, biceps tendon; G, glenoid; SAL, superoanterior labrum; SPL, superoposterior labrum. A lateral view of the von Mises strain distribution over the glenoid labrum is shown from a slightly inferior perspective. The inset represents the strain distribution across a section through the labrum expressed by the vertical black line with two arrow heads. The strain magnitude is shown by the scale at right.

Discussion

The hypothesis that humeral head translation, as can be seen in rotator cuff diseases, and tension on the biceps tendon may play a role in the development of labral pathology was supported by the rise in both superior labrum displacement and strain. The finite element model predicted a displacement profile that fell within 1 standard deviation of the labral displacements measured by cadaveric testing (Figure 2.3). The area of the highest predicted strain in the labrum also matched the clinical presentation of the most common superior labrum pathology (Figure 2. 5). The parametric sensitivity studies suggested that the labral strain pattern was not sensitive to the changes in material properties of 1 standard deviation for either the labrum or the articular cartilages (Figure 2.4). The average strain in each location was only affected by altering the constitutive model of the labrum (Figure 2.4). Therefore, it demonstrates strong potential for utilizing the finite element model to illuminate the mechanism of the superior labral tears secondary to rotator cuff tears.

Differences between the predicted and observed labral displacements may be explained by anatomic variations of the labrum. Firstly, the maximum difference between predicted and observed displacement occurred at the anchor of the biceps tendon and posterosuperior labrum (Figure 2.4). The biceps anchor on the superior labrum has been reported to have a highly variable morphology due to age-induced morphological adaptation.[35,36,37] Moreover, the attachment of the biceps tendon was slightly posterior in the specimen used for the current finite element model compared with the specimens used for cadaveric testing. Thus, the posterosuperior labrum would experience higher loads and displacement during biceps loading. Secondly, most values predicted by the finite element model were greater than the measures of displacement except for the 20º and 40º locations (Figure 2.4). This is explained by the relatively

small morphological volume of the anterosuperior labrum tissue in the specimen for the current finite element model. The radial thickness of the labrum at 20º and 40º in the shoulder used for modeling was (3.1 mm) compared with the thickness of the labrum (7.8 ± 1.3 mm) reported in the literature.[27,32] Thus, the force must pass through a smaller cross sectional area of tissue leading to higher tissue strains. Consequently, these results suggest that the displacement response of the labrum to superior humeral head translations is sensitive to labrum morphology and the attachment site of the biceps tendon.

This study suggests that the biceps tension may also serve an important role in labral tears. With biceps loading, the location of the maximum labral displacement moved from the anterior to posterior attachment of the biceps tendon (Figure 2.4). The location of the maximum displacement caused by biceps tension corresponds to the clinical description of a superior labral tear, which runs from the anterior side to the posterior side in the superior labrum.[38] The variability in the experimental data increased due to the biceps tension (Figure 2.4). It demonstrates that the direction of the load vector and the attached location of the biceps tendon may significantly affect labral behavior. This argument is supported by reports that the direction of biceps tension creates significant differences in the generation of superior labral tear[39] and that the anchor location of the biceps tendon influences the location of high stress on the labrum.[13]

Variation in constitutive models resulted in similar strain profiles, which shows the robustness of the current finite element model for predicting the strain response of the labrum. The strain pattern was not affected by changes in the constitutive models for either the labrum or the articular cartilages, or by changes of 1 standard deviation in the moduli for either tissue. The alteration of the constitutive model for the labrum from the hyperelastic to the elastic model, however, reduced the value of the labral strain. This finding is reasonable since, for the same

Young's modulus under the same stress conditions, the strain on hyperelastic material would exceed that on elastic material due to the toe region in the hyperelastic response.

The strain distribution predicted by the validated finite element model compares favorably with those of clinical and the experimental studies. The model predicts the region of the highest strain on the labrum at the interface with the glenoid cartilage and glenoid bone from approximately -20° to +40°. This high-strain region also extended through the labrum from the interface to the free surface in the radial direction. The area of the highest strain matched the location of the initial superior labral tear, and the strain distribution within the labrum in the radial direction corresponds with the most common type-II superior labral tear (Figure 2.5). The maximum strain with the current loading condition was approximately 17%. Cadaveric studies on the effects of shoulder instability during overhead throwing measured maximum strains in the labrum of approximately 24%.[14] The average strain for stable versus unstable shoulders was 10% and 17%, respectively. A previous computational labral model reported strains of 14% at 3 mm without consideration of the biceps tension, after conversion from a logarithmic strain to the von Mises strain.[16] In contrast, the mean strain at failure was reported for the human shoulder labrum as approximately 40%,[22] and from the human hip labrum as approximately 50%.[40] These failure strains are much higher than the strains predicted by the current model. Therefore, both the pattern and the magnitudes of the predicted strain compare well with those reported by previous studies.

Some assumptions were made regarding geometry and material properties during the development of the current finite element model. The appearance of the labrum in micro-CT images is similar to the surrounding soft tissues, necessitating identification of the boundary of the labrum by surgeons. Nevertheless, there is still a potential impact of error in labeling of the

labrum.[15] In addition, we used previously published data for determining material properties, but the reported material parameters show great variation among studies and among samples within those studies, which could have caused errors in estimating the value of the strain in the labrum. Overall these errors may affect the magnitude of the strain predicted by the model. However, we have shown that they have minimal impact on the relative distribution of strain in the labrum.

This finite element model correlated well with the experimental measures and predicted labral strains consistent with superior labral pathology. The model results demonstrate that increasing both biceps tension and superior humeral head translation also increased the labral displacement. Thus, computer models may provide further insight into the mechanism of labral injury as a function of biceps tension and superior humeral head translation.

References

1. Duke Orthopaedics, Wheeless' Textbook of Orthopaedics. Rotator cuff tears: Frequency of tears. Available at: http://www.wheelessonline.com/ortho/rotator_cuff_tears_frequency_of_tears. Accessed 31 May 2013.

2. Kim, T.K., Queale, W.S., Cosgarea, A.J., McFarland, E.G., 2003. Clinical features of the different types of SLAP lesions: an analysis of one hundred and thirty-nine cases. Journal of Bone and Joint Surgery (American) 85-A, 66-71.

3. Soslowsky, L.J., Flatow, E.L., Bigliani, L.U., Mow, V.C., 1991. Articular geometry of the glenohumeral joint. Clinical Orthopaedics and Related Research 285, 181-190.

4. Lippitt, S.B., Vanderhooft, J.E., Harris, S.L., Sidles, J.A., Harryman, D.T., 2nd, Matsen, F.A., 3rd, 1993. Glenohumeral stability from concavity-compression: A quantitative analysis. Journal of Shoulder and Elbow Surgery 2, 27-35.

5. Halder, A.M., Kuhl, S.G., Zobitz, M.E., Larson, D., An, K.N., 2001. Effects of the glenoid labrum and glenohumeral abduction on stability of the shoulder joint through concavity-compression. Journal of Bone and Joint Surgery 83(A), 1062-1069.

6. Keener, J.D., Wei, A.S., Kim, H.M., Steger-May, K., Yamaguchi, K., 2009. Proximal humeral migration in shoulders with symptomatic and asymptomatic rotator cuff tears. Journal of Bone and Joint Surgery (American) 91, 1405-1413.

7. Mura, N., O'Driscoll, S.W., Zobitz, M.E., Heers, G., Jenkyn, T.R., Chou, S.M., Halder, A.M., An, K.N., 2003. The effect of infraspinatus disruption on glenohumeral torque and superior migration of the humeral head: a biomechanical study. Journal of Shoulder and Elbow Surgery 12, 179-184.

8. Yamaguchi, K., Sher, J.S., Andersen, W.K., Garretson, R., Uribe, J.W., Hechtman, K., Neviaser, R.J., 2000. Glenohumeral motion in patients with rotator cuff tears: a comparison of asymptomatic and symptomatic shoulders. Journal of Shoulder and Elbow Surgery 9, 6-11.

9. Levine, W.N., Arroyo, J.S., Pollock, R.G., Flatow, E.L., Bigliani, L.U., 2000. Open revision stabilization surgery for recurrent anterior glenohumeral instability. American Journal of Sports Medicine 28, 156-160.

10. Tuoheti, Y., Itoi, E., Minagawa, H., Yamamoto, N., Saito, H., Seki, N., Okada, K., Shimada, Y., Abe, H., 2005. Attachment types of the long head of the biceps tendon to the glenoid labrum and their relationships with the glenohumeral ligaments. Arthroscopy 21, 1242-1249.

11. Vangsness, C.T., Jr., Jorgenson, S.S., Watson, T., Johnson, D.L., 1994. The origin of the long head of the biceps from the scapula and glenoid labrum. An anatomical study of 100 shoulders. Journal of Bone and Joint Surgery (British) 76, 951-954.

12. Youm, T., ElAttrache, N.S., Tibone, J.E., McGarry, M.H., Lee, T.Q., 2009. The effect of the long head of the biceps on glenohumeral kinematics. Journal of Shoulder and Elbow Surgery 18, 122-129.

13. Yeh, M.L., Lintner, D., Luo, Z.P., 2005. Stress distribution in the superior labrum during throwing motion. American Journal of Sports Medicine 33, 395-401.

14. Rizio, L., Garcia, J., Renard, R., Got, C., 2007. Anterior instability increases superior labral strain in the late cocking phase of throwing. Orthopedics 30, 544-550.

15. Drury, N.J., Ellis, B.J., Weiss, J.A., McMahon, P.J., Debski, R.E., 2010. The impact of glenoid labrum thickness and modulus on labrum and glenohumeral capsule function. Journal of Biomechanical Engineering 132, 121003.

16. Gatti, C.J., Maratt, J.D., Palmer, M.L., Hughes, R.E., Carpenter, J.E., 2010. Development and validation of a finite element model of the superior glenoid labrum. Annals of Biomedical Engineering 38, 3766-3776.

17. Ellis, B.J., Debski, R.E., Moore, S.M., McMahon, P.J., Weiss, J.A., 2007. Methodology and sensitivity studies for finite element modeling of the inferior glenohumeral ligament complex. Journal of Biomechanics 40, 603-612.

18. Debski, R.E., Weiss, J.A., Newman, W.J., Moore, S.M., McMahon, P.J., 2005. Stress and strain in the anterior band of the inferior glenohumeral ligament during a simulated clinical examination. Journal of Shoulder and Elbow Surgery 14, 24S-31S.

19. Henak, C.R., Ellis, B.J., Harris, M.D., Anderson, A.E., Peters, C.L., Weiss, J.A., 2011. Role of the acetabular labrum in load support across the hip joint. Journal of Biomechanics 44, 2201-2206.

20. Huang, C.Y., Stankiewicz, A., Ateshian, G.A., Mow, V.C., 2005. Anisotropy, inhomogeneity, and tension-compression nonlinearity of human glenohumeral cartilage in finite deformation. Journal of Biomechanics 38, 799-809.

21. Quapp, K.M., Weiss, J.A., 1998. Material characterization of human medial collateral ligament. Journal of Biomechanical Engineering 120, 757-763.

22. Smith, C.D., Masouros, S.D., Hill, A.M., Wallace, A.L., Amis, A.A., Bull, A.M., 2008. Tensile properties of the human glenoid labrum. Journal of Anatomy 212, 49-54.

23. Weiss, J.A., Maker, B.N., Govindjee, S., 1996. Finite element implementation of incompressible, transversely isotropic hyperelasticity. Comput Method Appl M 135, 107-128.

24. Carpenter, J.E., Wening, J.D., Mell, A.G., Langenderfer, J.E., Kuhn, J.E., Hughes, R.E., 2005. Changes in the long head of the biceps tendon in rotator cuff tear shoulders. Clinical Biomechanics (Bristol, Avon) 20, 162-165.

25. McGough, R.L., Debski, R.E., Taskiran, E., Fu, F.H., Woo, S.L., 1996. Mechanical properties of the long head of the biceps tendon. Knee Surgery, Sports Traumatology, Arthroscopy 3, 226-229.

26. Clavert, P., Zerah, M., Krier, J., Mille, P., Kempf, J.F., Kahn, J.L., 2006. Finite element analysis of the strain distribution in the humeral head tubercles during abduction: comparison of young and osteoporotic bone. Surgical and Radiologic Anatomy 28, 581–587.

27. Carey, J., Small, C.F., Pichora, D.R., 2000. In situ compressive properties of the glenoid labrum. Journal of Biomedical Materials Research 51, 711-716.

28. Anglin, C., Tolhurst, P., Wyss, U.P., Oichora, D.R., 1999. Glenoid cancellous bone strength and modulus. Journal of Bioemechanics 32, 1091-1097.

29. Lazarus, M.D., Sidles, J.A., Harryman, D.T., 2nd, Matsen, F.A., 3rd, 1996. Effect of a chondral-labral defect on glenoid concavity and glenohumeral stability. A cadaveric model. Journal of Bone and Joint Surgery (American) 78, 94-102.

30. Andarawis-Puri, N., Ricchetti, E.T., Soslowsky, L.J., 2009. Rotator cuff tendon strain correlates with tear propagation. Journal of Bioemechanics 42, 158-163.

31. Erdemir, A., Guess, T.M., Halloran, J., Tadepalli S.C., Morrison, T.M., 2012. Considerations for reporting finite element analysis studies in biomechanics. Journal of Biomechanics 45, 625-633.

32. Smith, C.D., Masouros, S.D., Hill, A.M., Wallace, A.L., Amis, A.A., Bull, A.M., 2009. The compressive behavior of the human glenoid labrum may explain the common patterns of SLAP lesions. Arthroscopy 25, 504-509.

33. Buchler, P., Ramaniraka, N.A., Rakotomanana, L.R., Iannotti, J.P., Farron, A., 2002. A finite element model of the shoulder: application to the comparison of normal and osteoarthritic joints. Clinical Biomechanics (Bristol, Avon) 17, 630-639.

34. Cohen, B., Gardner, T.R., Ateshian, G.A., 1993. The influence of transverse isotropy on cartilage indentation behavior. A study of the human humeral head. In: Transactions of the Annual Meeting of the Orthopaedic Research Society (February 15-18, 1993, San Francisco), vol. 18, p. 185.

35. Clavert, P., Kempf, J.F., Wolfram-Gabel, R., Kahn, J.L., 2005. Are there age induced morphologic variations of the superior glenoid labrum? About 100 shoulder arthroscopies. Surgical and Radiologic Anatomy 27, 385–388.

36. Costa Ado, S., Leite, J.A., Melo, F.E., Guimaraes, S.B., 2006. Biomechanical properties of the biceps-labral complex submitted to mechanical stress. Acta Cirurgica Brasileira 21, 214-218.

37. Healey, J.H., Barton, S., Noble, P., Kohl, H.W., 3rd, Ilahi, O.A., 2001. Biomechanical evaluation of the origin of the long head of the biceps tendon. Arthroscopy 17, 378-382.

38. Snyder, S.J., Banas, M.P., Karzel, R.P., 1995. An analysis of 140 injuries to the superior glenoid labrum. Journal of Shoulder and Elbow Surgery 4, 243-248.

39. Shepard, M.F., Dugas, J.R., Zeng, N., Andrews, J.R., 2004. Differences in the ultimate strength of the biceps anchor and the generation of type II superior labral anterior posterior lesions in a cadaveric model. American Journal of Sports Medicine 32, 1197-1201.

40. Ishiko, T., Naito, M., Moriyama, S., 2005. Tensile properties of the human acetabular labrum—The first report. Journal of Orthopaedic Research 23, 1448-1453.

CHAPTER III

EFFECTS OF BICEPS TENSION AND SUPERIOR HUMERAL HEAD TRANSLATION ON THE SUPERIOR GLENOID LABRUM

(Submitted to the Journal of Orthopaedic Research)

Introduction

Pathologic changes of the superior shoulder labrum are common, yet poorly understood. The most common type of pathology is a fraying or partial tearing of the labrum, coined a type-I tear by Snyder et al in 1995.[1] However detachment of the labrum from the superior glenoid bone, classified as a type-II tear, is considered the most common symptomatic injury. These injuries are thought to occur from sudden, excessive loads or from repetitive micro-trauma to the labrum as a result of loading from the long head of the biceps tendon or from superior translation of the humeral head. Tears in the superior labrum are most commonly seen in association with rotator cuff tears, where they may be secondary to pathologic joint loading which occurs as a result of the loss of rotator cuff function.[2] They can also occur in athletes or laborers with high loads across the joint and in the long head of the biceps tendon.

Understanding the factors leading to labral tears would better inform current treatments, which include repair, partial removal, or biceps tendon detachment, for patients with these conditions. However, the pathomechanics of these tears and the relationship to humeral head translation and loading of the biceps tendon are unclear. It has not been possible to adequately study the interaction of these factors *in vivo* or in a cadaveric model, making it an appropriate application for a computational model. This study reports on the further development and implementation of a finite element model of the superior labrum.

The purpose of this study was to understand the risk of injury to the superior glenoid labrum due to superior translation of the humeral head relative to the glenoid cavity (as can be seen in cases of rotator cuff tears) combined with tensile loading on the long head of the biceps tendon. We hypothesized that: (1) the regions of high strain in the labrum occur along a crescent in the mid-substance of the superior labrum corresponding to common superior labral lesions (types I and II); (2) increasing load on the long head of the biceps tendon causes increased strain in the labrum; and (3) the effect of humeral head translation on the increasing strain in the labrum is greater than the effect of biceps tension. These hypotheses are tested using a finite element model with material models that have been validated by comparison with mechanical testing of cadaveric specimens.[3,4] Risk for labral tearing is considered higher in areas of high tissue strains.

Methods

Development of a Finite element Model

A fresh frozen cadaveric shoulder (84-years-old) was dissected free of all soft tissue, leaving the scapula, humerus, labrum, long head of biceps tendon, and the articular cartilage intact. Using the GE eXplore Locus (GE Healthcare--Pre-Clinical Imaging, London, Canada) micro-CT system at a voxel size of 93 μm, the glenohumeral joint was scanned. The images were reconstructed at a resolution of 186 μm using a cone-beam back-projection algorithm. Segmentation and three-dimensional (3D) reconstruction were performed using commercial software (Amira 5.3, Visage Imaging, Inc., San Diego, CA). The 3D reconstructions were smoothed to remove poorly formed surfaces and segmentation artifacts.

The finite element mesh was generated from the reconstructed surface using a preprocessing tool (Hypermesh 10, Altair Engineering, Inc., Troy, MI, USA) and previously validated threshold settings.[3,4] The bones were modeled using rigid quadrilateral shell elements. The cartilages, labrum, and biceps tendon were converted to hexahedral, solid elements. Solid elements were added to the distal end of the biceps tendon to extend the tendon from the site of attachment on the labrum over the head of the humerus and through the bicipital groove (Figure 3.1). Mesh densities were determined by convergence studies.[4]

The labrum was modeled as transversely, isotropic, hyperelastic material[5,6] with four Young's moduli (21.3, 15.4, 19.3, and 20.9 MPa for superior, anterior, inferior, and posterior labrum, respectively).[4,6] The biceps tendon was modeled as an isotropic, hyperelastic material with an elastic modulus of 629 MPa based on previous cadaveric experiments on shoulders without rotator cuff pathology. [7] Cartilage was modeled as an isotropic elastic material (0.66 and 1.7 MPa for humerus and glenoid, respectively)[8,9] and bones were modeled as rigid materials.[10,11]

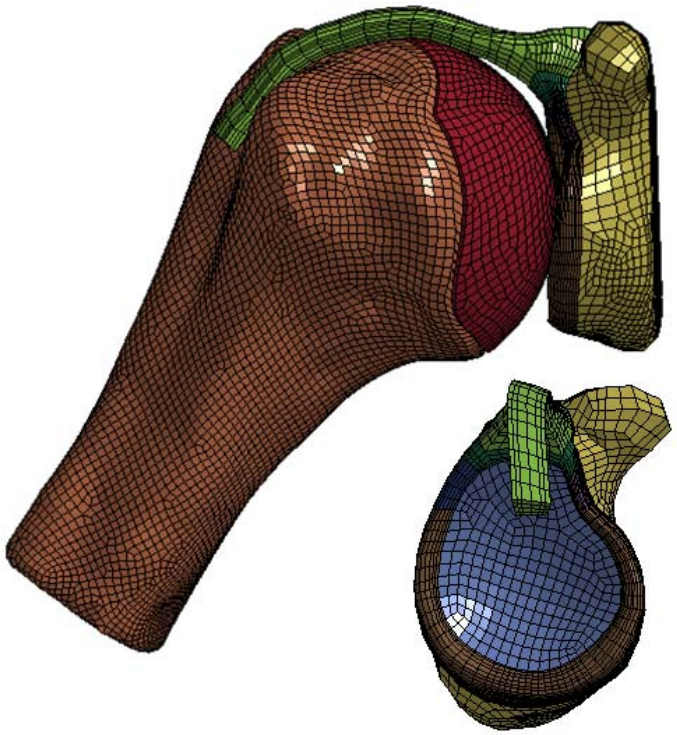

Figure 3.1 - A hexahedral finite element model of the glenohumeral joint, including the long head of biceps tendon. The humerus was positioned in 30˚ of glenohumeral abduction in the scapular plane with 0˚ humeral rotation. The humerus was shown in coronal view and was hidden in lateral view.

Loading Conditions

The humerus was positioned in 30˚ of glenohumeral abduction in the scapular plane with neutral humeral rotation.[3] The medial surface of the glenoid was constrained in all six degrees of freedom. A 50-N compressive load was applied to the humeral head in the medial direction to seat the humerus in the glenoid cavity.[3,12] We considered this location the zero position of the humerus. Next, the humerus was held at the zero position and the desired tension was applied to the free end of the biceps tendon and directed along the force vector of the biceps muscle. While maintaining the compression and the biceps tension, the humerus was superiorly translated up to 5 mm.[4] This amount of humeral head displacement was chosen to encompass the range of displacements encountered clinically in patients with massive rotator cuff disease.[13]

We tested four conditions for the biceps tension: 0 N, 22 N, 55 N, and 88 N. A 22 N load was chosen because it was shown to affect glenohumeral range of motion and kinematics.[14] A 55-N load was used because it represents the force of maximum isometric contraction calculated from physiologic cross-sectional area of the long head of the biceps muscle.[15] We also tested 88 N of tensile loading[16] to evaluate the effects of increased force generation during stretch of an activated muscle capable, or an eccentric contraction, when whole muscles are capable or resisting to 160% of the force from a maximal isometric contraction.[17]

Dynamic Analyses and Statistics

Analyses were performed using LS-DYNA/Explicit version mpp971d (Livermore Software Technology Corporation, Livermore, CA). All sliding interfaces were modeled using frictionless, surface-to-surface contact due to the low coefficient of friction in synovial joints.[18]

During biceps loading and humeral head translation, we predicted the von Mises strain since it is a scalar quantity representing the combined effect of all components of the material strain tensor and indicative of the energy required to distort the material. The strain for a cross section through the labrum was calculated by performing a volume-weighted average of the von Mises strains for the elements within that cross-sectional area.

A regression model was used to assess for main effects as well as interactions on the strain. The main effects were humeral head displacement, position along the labrum, and tension on the long head of the biceps tendon. Repeated measures one-way analyses of variance were then used to assess the significance of each effect. All statistical analyses were performed using SPSS Version 20 (IBM Corp, Armonk, New York) with the significance set at the 0.05 level.

Results

Finite element Predictions of Strain in the Labrum

The highest strain in the superior labrum occurred at the interface with the glenoid cartilage and glenoid bone along an arc from approximately -20° to +40° with respect to the inferior-superior vector (Figure 3.2d). The high-strain region also extended radially through the labrum from the cartilage interface surface to the free surface (Figure 3.2d, inset). This strain pattern corresponds well with an arthroscopic image of a type-II SLAP (superior labral anterior-posterior) lesion (Figure 3.3).

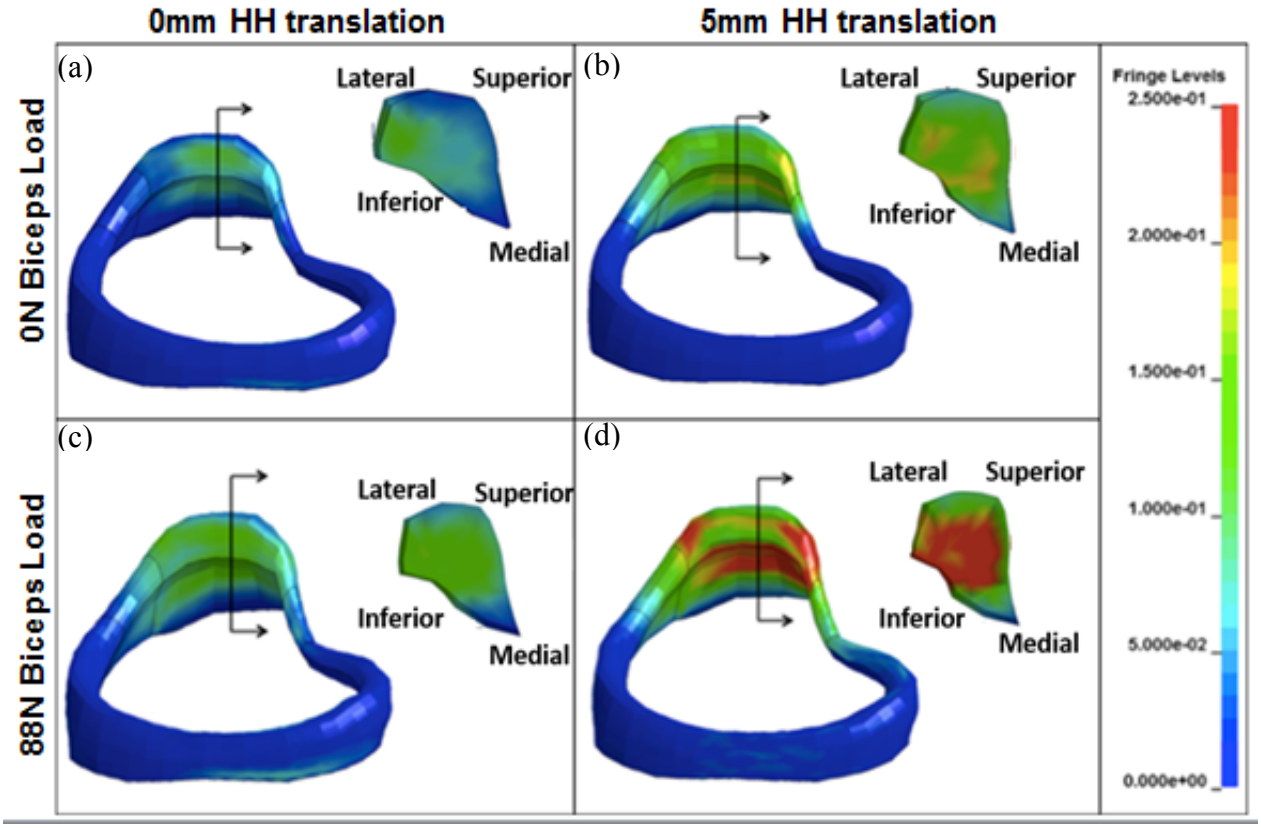

Figure 3.2 - Strain distribution after application of a 50 N compressive load on the humeral head with the following conditions of superior humeral head translation and biceps load: (A) 0 mm, 0 N; (B) 5 mm, 0 N; (C) 0 mm, 88 N; and (D) 5 mm, 88 N. A lateral view of the von Mises strain distribution over the glenoid labrum is shown from a slightly inferior perspective. The inset represents the strain distribution across a section through the labrum expressed by the vertical black line with two arrow heads. The strain magnitude is shown by the scale at right.

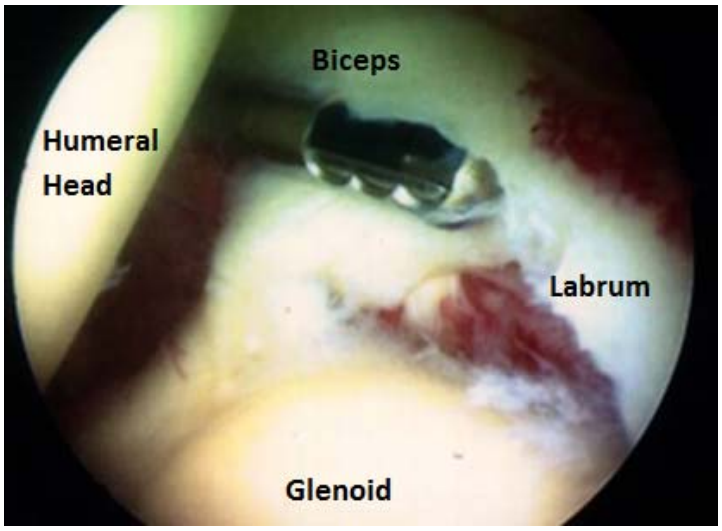

Figure 3.3 – Arthoscopic view from the same angle as Figure 3.2 showing that the strain patterns predicted by the model correlate well with arthroscopic observations of a type-II SLAP lesion.

Effect of Biceps Tension on Labrum Strain

When the load on the biceps was increased, strain in the superior labrum increased in the labrum (Figures 3.2 and 3.4). The high-strain region extended from the origin of the biceps on the superior surface of the labrum to the glenoid bone and cartilage interface on the inferior surface of the labrum (Figures 3.2c and 3.2d, insets). Increasing the biceps load caused an increase in the strain magnitude in the circumferential direction and involved more of the superior labrum from -40º to +40º (Figures 3.2c and 3.2d). The highest strain was located at 0˚ with respect to the inferior-superior vector (Figure 3.4). Increasing the biceps tension from 0 N to 88 N increased the strain by a factor of 27% at 0 mm and 40% at 5 mm of humeral head displacement (Figure 3.4). The region of the labrum with the highest strain was independent of the magnitude of the biceps load (Figure 3.4).

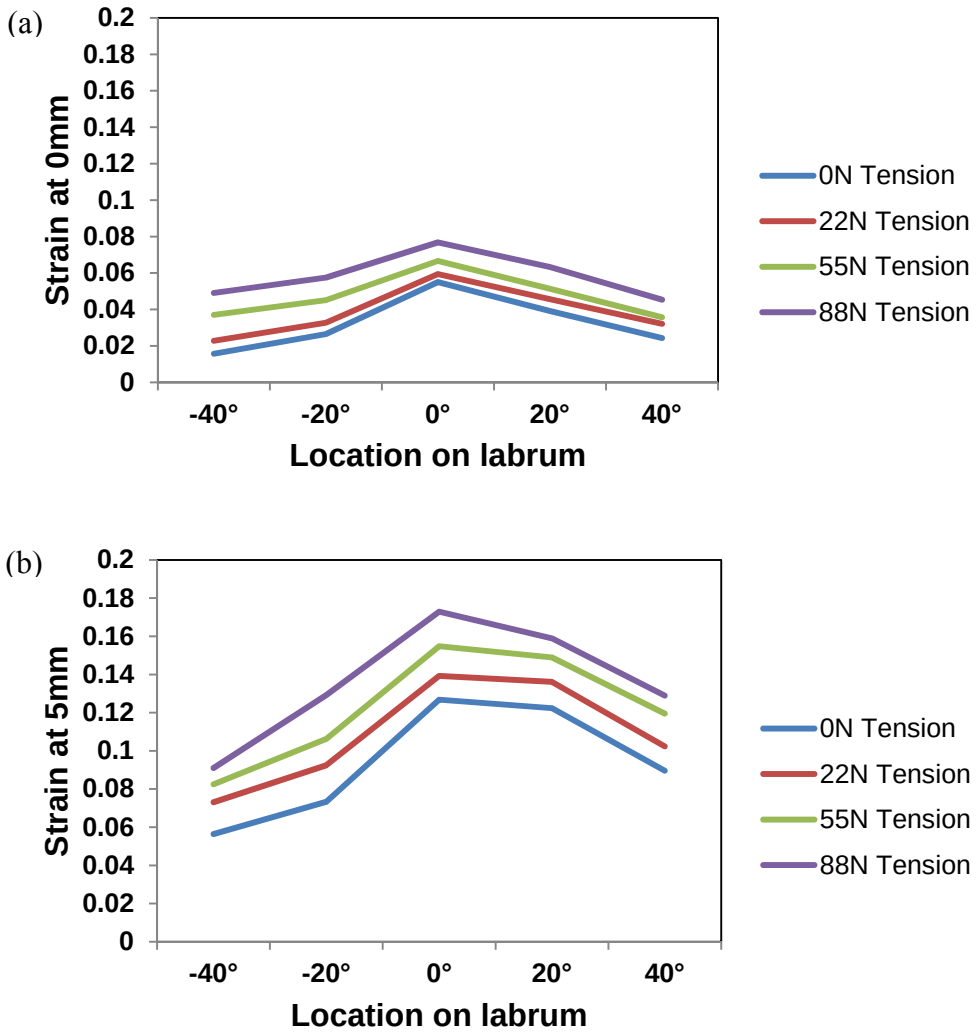

Figure 3.4 - Strain in labrum due to tension on the biceps tendon at (a) 0 mm and (b) 5 mm of humeral head translation.

Effect of Superior Humeral Head Translation

Increasing the translation of the humeral head in the superior direction caused an increase in the strain in the superior labrum (Figures 3.4 and 3.5). We observed the strain at 0˚ along the inferior-superior vector, coincident with the area of the highest strain (Figure 3.5). Translation of the humeral head from 0 mm to 5 mm resulted in an increase in strain in excess of 100% for each magnitude of long head of biceps load (Figure 3.5).

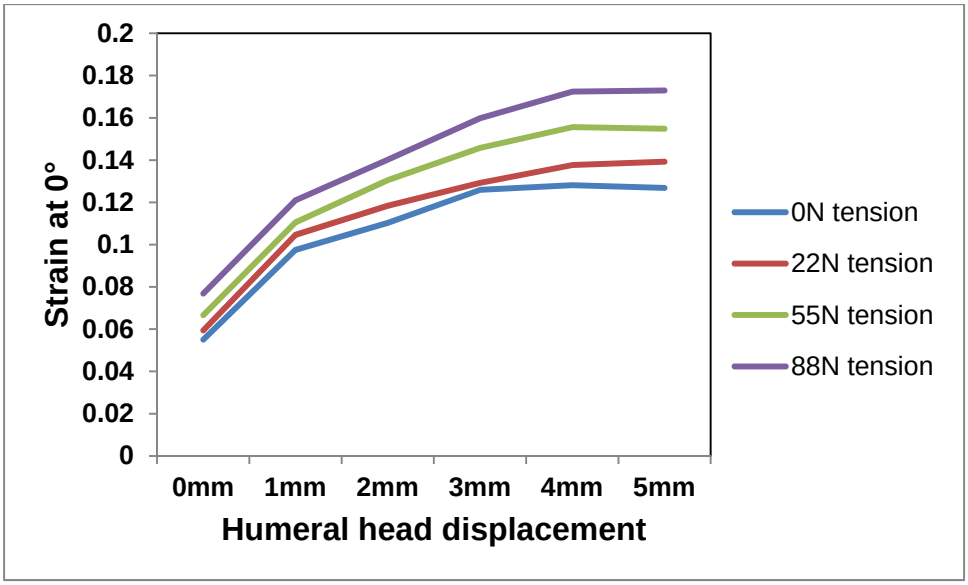

Figure 3.5 – Von-Mises Strain in labrum due to humeral head translation.

Statistical Analysis

The strain predicted at each cross section through the labrum in the radial direction was significantly affected by superior translation of the humeral head ($p < 0.001$), position along the labrum ($p < 0.001$), and biceps load ($p = 0.002$). A linear regression analysis for predicting the average strain in a cross section through the labrum resulted in R = 0.739. The model was strain = 0.04 + 0.013 × humeral head translation [mm] + 0.00381 × biceps tension [N] + 0.000332 × location along the labrum [degrees].

Discussion

The purpose of our study was to predict the risk of injury to the superior labrum, which may occur in patients with rotator cuff tears and from loading of the long head of biceps tendon. Pathologic loading of the labrum was simulated by superior humeral translation while the risk for labral tear was determined by predicting strain in the superior labrum with a constant tension applied to the long head of the biceps tendon. The highest strains in the labrum were found along a crescent in the mid-substance of the superior labrum in the area where these tears are most commonly seen clinically (Figure 3.2). Increasing load on the biceps tendon correspondingly increased strain in the labrum (Figures 3.4 and 3.5). The effect of humeral head translation on increasing the labral strain is greater than the effect of the biceps tendon tension. Therefore, this study supports the mechanistic hypothesis that a superior lesion (SLAP tear) may occur as a result of superior migration of the humeral head regardless of amount of the biceps load.

The current study supports experimental evidence that an unstable shoulder increases the susceptibility of the labrum to injury. To generate the conditions for an unstable shoulder, Rizio and colleagues generated a Bankart lesion, an avulsion of the anteroinferior glenoid labrum, and then sutured the damaged tissue.[19] They found that increased instability caused greater strain on the labrum. Similarly, the current model shows that the strain in the superior labrum increased with increasing humeral head migration in the superior direction (Figures 3.4 and 3.5). In the current model, a compressive force between the humeral head and the glenoid cavity combined with superior translation of the humeral head causes compression and shear of the superior labrum at the interface with the glenoid cartilage and glenoid bone. The load directed medially by the humeral head combined with tension from the biceps tendon directed superiorly results in a plane of high strain at the origin of the biceps tendon on the superior glenoid bone (Figure 3.2).

This loading pattern consisting of combined shearing and avulsion loads would result in localized detachment of the labrum from the underlying glenoid consistent with a type-II SLAP lesion (Figure 3.3)

The finite element model predicts that the tension of the biceps tendon is transferred and dissipated by the labrum along pathways in the radial and circumferential direction. First, the labrum transfers the load from the biceps tendon to the glenoid bone and cartilage on the superior edge of the glenoid in the radial direction. At 50 N of compressive force between the humeral head and glenoid and no biceps load prior to superior translation of the humeral head, the strain field in the cross section of the labrum is relatively low (Figure 3.2a, inset). When the load on the biceps is increased under these conditions, strain also increases in the cross section of the labrum (Figure 3.2c, inset). Therefore the predicted strain field demonstrates a loading pathway from the attachment of the biceps on the superior labrum to the glenoid bone and cartilage interface on the inferior labrum (Figure 3.2c, inset). Similarly, comparing 0 N of biceps load at 5 mm of humeral head translation (Figure 3.2b, inset) with 88 N of load at 5 mm of translation (Figure 3.2d, inset), there is a high-strain pathway from the origin of the biceps tendon on the superior surface of the labrum to the interface of the inferior surface of the labrum with the glenoid bone and cartilage. Second, the biceps force is also transferred from the biceps attachment site circumferentially through the labrum in both the anterior and posterior directions. At 0 N of biceps load and 50 N of compressive force (Figures 3.2a and 3.2b), the model predicted low levels of strain in the circumferential direction from -20º to +20º. Increasing the biceps load causes an increase in the strain magnitude in the circumferential direction and involves more of the superior labrum from -40º to +40º (Figures 3.2c and 3.2d).

While the strain magnitudes predicted by the current model using physiologic loading levels are lower than what would be expected to result in an acute tear, they do support the theory of repetitive micro-trauma, also known as tissue fatigue, in the development of superior labrum pathology. In this scenario, repetitive loads below the one-time failure level result in tissue tearing over time due to accumulated damage. Previous cadaveric studies on the effects of shoulder instability during overhead throwing measured labrum strains up to 24%. The average strain for stable versus unstable shoulders was 10% and 17%, respectively.[19] A previous computational model of the labrum reported mean strains of 14% at 3 mm of humeral head displacement after conversion from logarithmic strain to Green strain.[3] The current model predicts a mean strain of 13% at 3 mm and 14% at 5 mm of humeral head displacement in the absence of a biceps tendon. With a biceps load of 88 N, the peak mean strain was 17% at 5 mm of humeral head displacement. Therefore, the strain magnitudes predicted by the current model compare well with those reported by previous computational and experimental studies. However, the mean strain at failure for the labrum from human hip is approximately 50%.[20] Similarly, the failure strain for isolated tissue samples of labrum from human shoulders is approximately 40%.[6] These failure strains are much higher than the peak localized strains predicted by the current model that range from 17% at 0 N biceps load to 25% at 88 N biceps load. Consequently, this model suggests that repetitive micro-trauma or tissue fatigue would be necessary to cause a mid-substance failure of the labrum. It is also possible that single loads at levels well above those modeled could lead to failure strains in the labrum and at the bone labrum junction.

The higher strain on the anterior side compared to the posterior side (Figure 3.4) can be explained from anatomic characteristics of the specimen used to construct the finite element model and the path of humeral head migration. The volume of labrum on the posterior side was

larger than that on the anterior side in our specimen. The radial thickness of the anterosuperior labrum in the specimen was also smaller (3.1 mm) compared with the thickness (7.8 ± 1.3 mm) reported in the literature.[8] Consequently, the force must pass through a smaller cross-sectional area of tissue leading to higher tissue stresses and strains. Meanwhile, the larger volume of the posterosuperior labrum would lead to smaller stresses and strains. In addition, if the humeral head were translated in a more posterior-superior direction, the posterior labrum likely would have registered higher strain levels.

The strain pattern was mainly affected by the magnitude of humeral head translation. The shape of the strain curve as a function of humeral head translation (Figure 3.5) is determined by the size of the contact surface between the humeral head and the labrum. At 0 mm of humeral head translation, the contact area is primarily on the glenoid cartilage and the superior labrum. With increasing humeral head translation, the contact area moves superiorly onto the superior labrum. For low biceps loads, the periphery of the labrum is relatively unconstrained so the labrum does not conform to the contour of the humeral head. Consequently, the labrum is displaced superiorly and medially in the direction of its free surface. As the load on the biceps tendon is increased, the superior labrum is pulled towards the humeral head. For the case of 88 N of tensile load on the biceps, the load is sufficient to constrain the superior labrum to conform to the contour of the humeral head. Increased conformity between the humeral head and the superior labrum increases the contact area between the humeral head and the labrum, which in turn increases the strain in the labrum. The model also demonstrated that increasing the load on the biceps tendon from 0 N to 88 N increased the total strain in the labrum by 27% at 0 mm and 40% at 5 mm of humeral head displacement (Figure 3.4).

There are a number of limitations to this study. The interfaces of the labrum with the glenoid bone, cartilage, and capsule are complex. So it was necessary to make simplifying assumptions to develop a finite element model. The properties of the superior labrum are not based on a detailed representation of the labrum microstructure, even though we used the latest published data for determining material properties.[6] Errors in approximating the stiffness of the material would affect the magnitude of strain, but not the overall tendency of the strain pattern. The current model also assumes that the collagen fibers of the superior labrum are oriented primarily circumferentially. A more complex collagen fiber network particularly at the origin of the biceps tendon would reduce the strain in the mid-substance of the labrum causing higher stresses at the interface of the labrum with the superior glenoid.

A third limitation of the model is the response of the long head of biceps muscle. The biceps tendon travels superiorly over the head of humerus before attaching to the muscle. Depending on the orientation of the humeral head with respect to the glenoid, the biceps tendon may experience a stretch up to twice the displacement of the humeral head. When skeletal muscle is activated and stretched, an eccentric contraction, the muscle force may increase by 60% compared to the isometric load.[17] However, the long head of biceps muscle is biarticular acting across both the elbow and glenohumeral joints. The positions of both joints determine the initial length, stretch, and force of the muscle. Rather than simulate the dynamic changes in muscle force, we demonstrate the response of the labrum over a range of humeral head translations (0 mm to 5 mm) as well as a range of muscle forces that span 0% to 160% of peak isometric force in muscle. Therefore this study predicts the trends in the stress-strain state for the labrum for likely physiologic ranges of biceps loads and humeral head displacements but does not predict a specific biceps load or loading pathway as a function of humeral head position.

In summary, the interactions among biceps loading, humeral translation and labral tissue mechanics were tested with an anatomically accurate model of the glenohumeral joint. Under physiologic conditions, superior translation of the humeral head results in higher labral strains than does biceps tendon loading. The predicted strain pattern is consistent with tears in the superior labrum described clinically. Maximum predicted strain lower than the failure strain suggests that repetitive micro-trauma or tissue fatigue rather than a single loading event may be necessary to cause a mid-substance failure of the labrum.

References

1. Snyder, S.J., Banas, M.P., Karzel, R.P., 1995. An analysis of 140 injuries to the superior glenoid labrum. Journal of Shoulder and Elbow Surgery 4, 243-248.

2. Kim,T.K., Queale, W.S., Cosgarea, A.J., McFarland, E.G., 2003. Clinical features of the different types of SLAP lesions: an analysis of one hundred and thirty-nine cases. Journal of Bone and Joint Surgery (American) 85-A:66-71.

3. Gatti, C.J., Maratt, J.D., Palmer, M.L., Hughes, R.E., Carpenter, J.E., 2010. Development and validation of a finite element model of the superior glenoid labrum. Annals of Biomedical Engineering 38, 3766-3776.

4. Hwang, E.J., Carpenter, J., Hughes, R., Palmer, M.L., 2014. Shoulder labral pathomechanics with rotator cuff tears. Accepted. Journal of Biomechanics.

5. Weiss, J.A., Maker, B.N., Govindjee, S., 1996. Finite element implementation of incompressible, transversely isotropic hyperelasticity. Computer Methods in Applied Mechanics and Engineering 135, 107-128.

6. Smith, C.D., Masouros, S.D., Hill, A.M., Wallace, A.L., Amis, A.A., Bull, A.M., 2008. Tensile properties of the human glenoid labrum. Journal of Anatomy 212, 49-54.

7. Carpenter, J.E., Wening, J.D., Mell, A.G., Langenderfer, J.E., Kuhn, J.E., Hughes, R.E., 2005. Changes in the long head of the biceps tendon in rotator cuff tear shoulders. Clinical Biomechanics 20, 162-165.

8. Carey, J., Small, C.F., Pichora, D.R., 2000. In situ compressive properties of the glenoid labrum. Journal of Biomedical Materials Research 51, 711-716.

9. Donzelli, P.S., Spilker, R.L., Ateshian, G.A., Mow, V.C., 1999. Contact analysis of biphasic transversely isotropic cartilage layers and correlations with tissue failure. Journal of Biomechanics 32, 1037-1047.

10. Anglin, C., Tolhurst, P., Wyss, U.P., Pichora, DR., 1999. Glenoid cancellous bone strength and modulus. Journal of Biomechanics 32, 1091-1097.

11. Clavert, P., Zerah, M., Krier, J.,Mille, P., Kempf, J.F., Kahn, J.L., 2006. Finite element analysis of the strain distribution in the humeral head tubercles during abduction: comparison of young and osteoporotic bone. Surgical and Radiologic Anatomy 28, 581-587.

12. Lippitt, S.B., Vanderhooft, J.E., Harris, S.L., Sidles, J.A., Harryman II, D.T., Matsen III, F.A., 1993. Glenohumeral stability from concavity-compression: A quantitative analysis. Journal of Shoulder and Elbow Surgery 2, 27-35.

13. Mura, N., O'Driscoll, S.W., Zobitz, M.E., Heers, G., Jenkyn, T.R., Chou, S.M., Halder, A.M., An, K., 2003. The effect of infraspinatus disruption on glenohumeral torque and superior migration of the humeral head: a biomechanical study. Journal of Shoulder and Elbow Surgery 12, 179-184.

14. Youm, T., ElAttrache, N.S., Tibone, J.E., McGarry, M.H., Lee, T.Q., 2009. The effect of the long head of the biceps on glenohumeral kinematics. Journal of Shoulder and Elbow Surgery 18, 122-129.

15. Su, W.R., Budoff, J.E., Luo, Z.P., 2010. The effect of posterosuperior rotator cuff tears and biceps loading on glenohumeral translation. Arthroscopy 26, 578-586.

16. Langenderfer, J., LaScalza, S., Mell, A., Capenter, J.E., Kuhn, J.E., Hughes, R.E., 2005. An EMG-driven model of the upper extremity and estimation of long head biceps force. Computers in Biolology and Medicine 35, 25-39.

17. McCully, K.K., Faulkner, J.A., 1985. Injury to skeletal muscle fibers of mice following lengthening contractions. Journal of Applied Physiology 59, 119-126.

18. Henak, C.R., Ellis, B.J., Harris, M.D., Anderson, A.E., Peters, C.L., Weiss, J.A., 2011. Role of the acetabular labrum in load support across the hip joint. Journal of Biomechanics 44, 2201-2206.

19. Rizio, L., Garcia, J., Renard, R., Got, C., 2007. Anterior instability increases superior labral strain in the late cocking phase of throwing. Orthopedics 30, 544-550.

20. Ishiko, T., Naito, M., Moriyama, S., 2005. Tensile properties of the human acetabular labrum-the first report. Journal of Orthopaedic Research 23, 1448-1453.

CHAPTER IV

EFFECT OF BICEPS TENSION ON THE TORN SUPERIOR GLENOID LABRUM

(In preparation for Journal of Sports Medicine)

Introduction

The lesion of the Superior Labrum extending from Anterior to Posterior (SLAP) is a traumatic tear in the superior glenoid labrum, which may include the attachment of the long head of the bicep tendon. This tear can contribute to significant pain and disability in the shoulder.[1,2] The SLAP tear is classified according to four or more subtypes.[3,4,5] Among them, the tear involving detachment of both the superior labrum and the biceps tendon from the glenoid has been reported as the most common lesion.[3,6,7,8]

In numerous biomechanical studies of the tear mechanism, both the motion of the humeral head and the traction on the biceps tendon have been generally implicated as predominant factors in SLAP tears. When SLAP tears were first described, it was hypothesized that they resulted from the traction imposed on the biceps tendon during repeated throwing movements.[9] Later, multiple mechanisms were suggested for the creation of the SLAP tear: the

combination of humeral head compression and the biceps tension[10]; the pinched and compressed glenohumeral joint with internal impingement[11]; and the pulled and twisted biceps tendon.[12]

However, there is still a knowledge gap concerning how the biceps tension affects the SLAP tear pathology, and thus the optimal treatment of the biceps tendon following the SLAP tear. By testing the labral strain at a specific phase during certain motions, most researchers agree that biceps tension causes the SLAP tear[13,14,15,16]. Therefore, the portions of an activity at high risk for generating a SLAP tear were identified. However, a governing principle for the effect of biceps tension on the initiation of a SLAP tear could not be determined. Moreover, none of those studies observed either the strain inside of the labrum tissue or the behavior of the labrum with an existing SLAP tear. Most experimental studies focus on the genesis of the SLAP tear, so theories on the propagation of SLAP tears were neither suggested nor tested. In addition, Costa et al. reported a simple traction of the biceps tendon does not play a role in the initiation of the SLAP tear.[17] The lack of clear understanding concerning the role of biceps tension on the SLAP tear mechanism leads to debates among surgeons on the proper treatment for the biceps tendon among the following: arthroscopic repair, debridement, tenodesis, tenotomy, or solely observation.[18, 19, 20, 21]

Therefore, the purpose of this study was to understand the role of the tension on the long head of the biceps tendon on the propagation of SLAP tears by studying the mechanical behavior of the torn superior glenoid labrum. We hypothesized that: (1) the regions of high strain in the torn labrum occur at the edge of the given tear; (2) increasing load on the long head of the biceps tendon causes increased strain in the torn labrum regardless of the tear size; and (3) the effect of the biceps tension on the increasing strain in the torn labrum is greater than that in the intact labrum. These hypotheses are tested by extending a validated finite element model[22] to

investigate the strain distribution inside of the labrum tissue. The extended model includes a glenoid labrum with SLAP tears of different sizes. The tear on the glenoid labrum is introduced to simulate detachment of the superior labrum including the detachment of the biceps tendon from the glenoid rim, the most common SLAP tear.[3,8]

Methods

Development of an Intact Model

The more detailed information about the development of an intact finite element model was provided by previous paper.[22] The scapula, humerus, labrum, long head of the biceps tendon, and the articular cartilages from a fresh frozen cadaveric shoulder were scanned to develop a three-dimensional finite element model of the glenohumeral joint having an intact glenoid labrum. The scanned micro CT images by GE eXplore Locus (GE Healthcare--Pre-Clinical Imaging, London, Canada) were segmented and smoothed into each tissue component using commercial software (Amira 5.3, Visage Imaging, Inc., San Diego, CA). Based on surface information of each tissue, the finite element mesh was generated by a preprocessing tool (Hypermesh 10, Altair Engineering, Inc., Troy, MI, USA). Mesh density and material properties were defined according to previously validated settings.[22] Shell elements were used for the bones and hexahedral elements for the soft tissues. At the lateral end of the biceps anchor-labrum complex, hexahedral elements were added to extend the tendon over the humeral head and through the bicipital groove (Figure 4.1). Bones were assumed as rigid materials[23,24] and cartilages were modeled as an isotropic elastic material (0.66 and 1.7 MPa for the humerus and the glenoid, respectively).[25,26] The glenoid labrum was sectioned into superior, anterior, inferior, and posterior labrum having four different elastic modulus (21.3, 15.4, 19.3, and 20.9 MPa, respectively)[22,27] and assumed as a transversely isotropic, hyperelastic material.[5,6] The behavior of the biceps tendon was expressed by an isotropic, hyperelastic material with an elastic modulus of 629 MPa.[28] All sliding interfaces were modeled using frictionless, surface-to-surface contact due to the low coefficient of friction in synovial joints.[29]

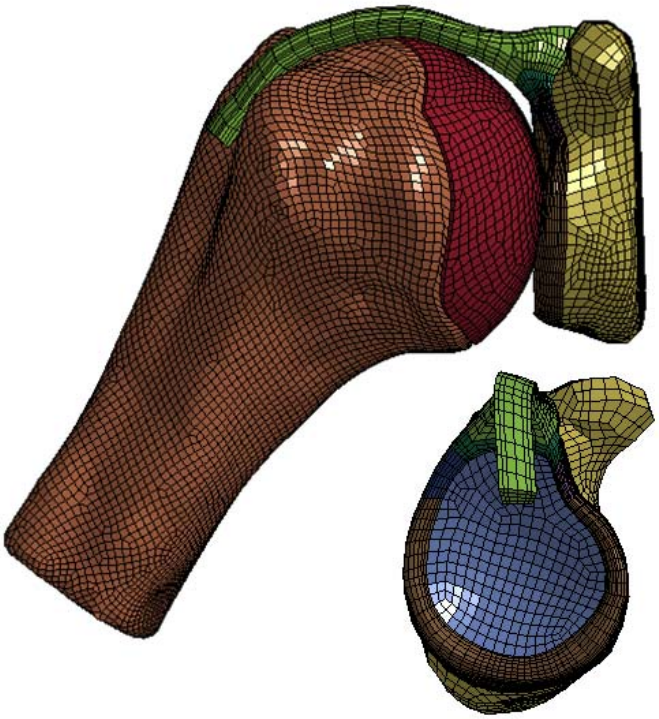

Figure 4.1 - A validated finite element model of the glenohumeral joint with SLAP tears introduced at the interface between the glenoid and the superior labrum.

Type II SLAP tear models

Type II SLAP, the most common SLAP, tear models were introduced in the intact model. Three different sizes of tears in the superior labrum were introduced at the interface with the glenoid rim along an arc (Figure 4.2). The small tear was introduced between -10° to +10° with respect inferior-superior vector.[4] The medium tear ran from -30° to +30°, [30,31] while the larger tear ran between -60° to +30°.[30] Tears were introduced by creating the physical separation between the desired portion of the superior labrum and the corresponding portion of the glenoid bone and cartilage. The shared nodes among the superior labrum and the glenoid rim in the intact model were duplicated to permit motion of the elements at the plane of separation. The other portions of the model including mesh density, boundary conditions, material properties, and contact definitions were not changed from the intact finite element model.

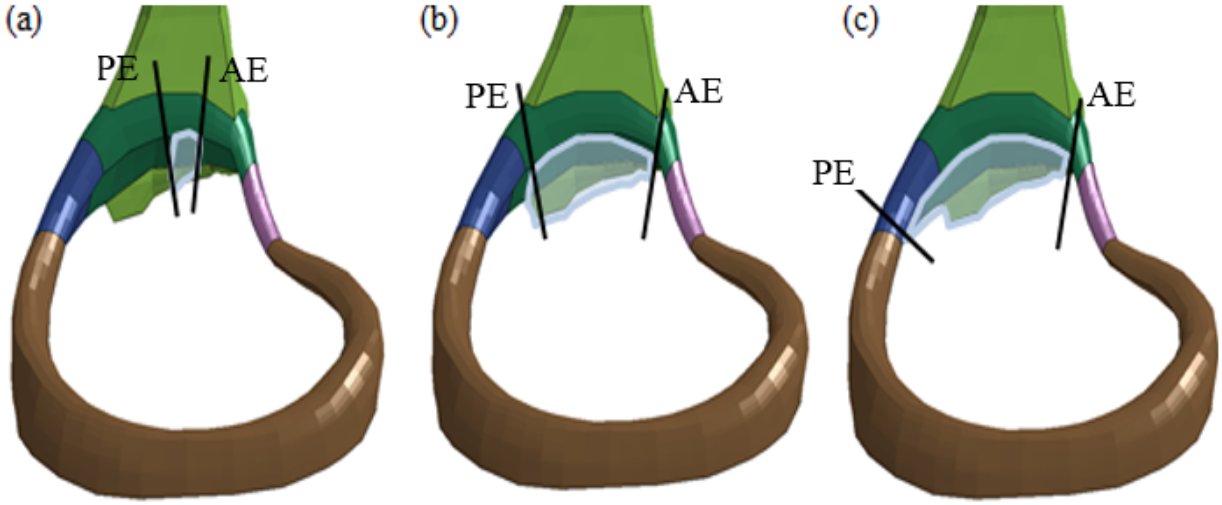

Figure 4.2 - The labrum component in the models of the glenohumeral joint showing (a) a small SLAP tear model; (b) a medium SLAP tear model; and (c) a large SLAP tear model. PE, posterior edge; AE, anterior edge of the SLAP tear. The light green is for biceps tendon. In this and following figures, the labrum is shown in a lateral view from a slightly inferior perspective.

Loading Conditions

The humerus was positioned in 30˚ of abduction in the scapular plane without humeral rotation.[32] 50 N of compressive force was applied to seat the head of the humerus in the glenoid cavity. At the same time, the desired tension was applied to the lateral end of the biceps tendon and directed along the force vector of the biceps muscle. Four different amounts of tensile forces to the long head of the biceps tendon were modeled, namely, 0 N, 22 N, 55 N, and 88 N. A tension of 22 N was chosen because it was shown to affect the range of motion and kinematics of the glenohumeral joint.[33] A tension of 55 N was chosen to represent the force of maximum isometric contraction calculated from physiologic cross-sectional area of the long head of the biceps muscle.[34] A tensile loading of 88 N[35] was chosen to simulate the maximum force during stretch of an activated muscle, or a lengthening contraction.[36]

Data Analysis

Analyses were performed using the FE solver, LS-DYNA/Explicit version mpp971d (Livermore Software Technology Corporation, Livermore, CA), and the statistical software, SPSS Version 20 (IBM Corp, Armonk, New York). The distribution of both the effective von Mises strain[37] and maximum-principal strain were observed.[38,39] The von Mises strain is a scalar quantity representing the combined effect of all components of the material strain tensor and indicative of the energy required to distort the material and was used to predict the site of failure.[40] The maximum-principal strain was measured because there is a direct positive relationship between an increase in maximum-principal strain and increase in tear size.[38] The von Mises strains were averaged to calculate the surface strain (along the contacting surface only) and the volume strain (within the all elements in the cross-sectional area through the labrum). All nodal strains in the contact surface were averaged within the specific interaction region. To compare the strains, the 0° position below the origin of the biceps tendon for the intact labrum and posterior edge for the SLAP tear were selected for observation. The posterior edge was chosen because the SLAP tear has been known to extend in posterior direction. The effect of biceps tension on the labral strain in each SLAP tear model was assessed. The strain in the labrum including a medium and a large SLAP tear was compared the strain in the labrum with no and a small SLAP tear by use of a paired t-test. The difference in the strain pattern of the intact labrum from that of the labrum having a small SLAP tear was also analyzed using a paired t-test. The significance level for all statistical analysis was 0.05.

Results

Predicted strain distribution in the torn labrum

The highest strain in the torn labrum was observed at the edge of the given SLAP tear regardless of the size of the tear (Figure 4.3). The location experiencing the high strain was matched with the edge of the given tear in the Figure 4.2. With larger size of the SLAP tear, the superior labrum also had a larger peak strain value. The strain distributions in other biceps loading conditions were similar to the strain contour shown in Figure 4.3.

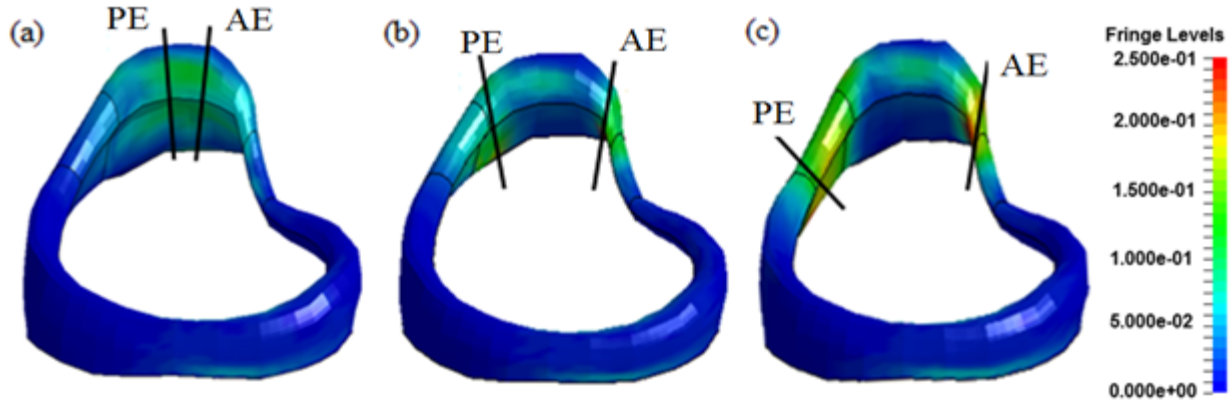

Figure 4.3 - The predicted maximum-principal strain distribution in the labrum with (a) a small; (b) a medium; and (c) a large SLAP tear finite element model under 22 N of biceps tension. PE, posterior edge; AE, anterior edge of the SLAP tear.

Effect of biceps tension on the labral strain

The highest labral strains were predicted for the highest biceps tension regardless of the size of the labrum tear (Figure 4.4). The effect of the biceps tension on the maximum-principal strain of the labrum including a medium or a large SLAP tear is significantly greater than the effect of biceps tension on the strain of the intact labrum or the labrum with a small tear. Under 0N of biceps tensile load, the predicted strains in all models are approximately 5% (Figure 4.4).

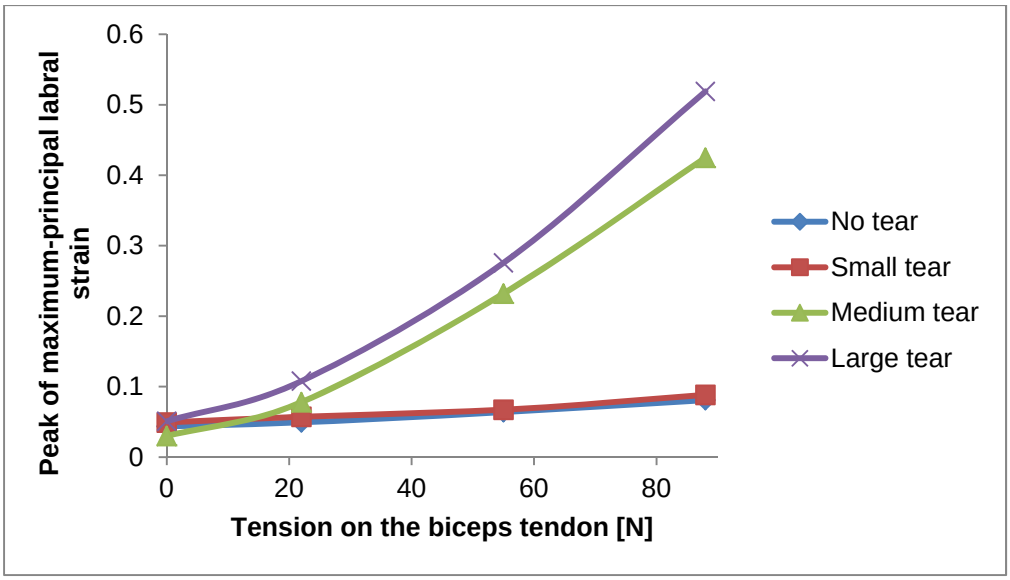

Figure 4.4 - The effect of the biceps tension on the peak of the maximum-principal strain measured at the posterior edge (PE) of the given SLAP tear in the glenoid labrum.

Effect of tear size on the labral strain

The behavior of the labrum tissue with a medium or a large SLAP tear was different from the small tear or no tear conditions (Figure 4.5 and Figure 4.6). The predicted von Mises strain distribution at the cross sectional area in the small SLAP tear model is more akin to the intact model than the medium and large tear models. The behavior of the labrum having a small tear was significantly related to that of intact labrum under all biceps loading conditions. In the labrum having a medium and a large SLAP tear (larger tear group), increasing biceps tension significantly increased von Mises strain. In the larger tear group, the surface strain was higher than the volume strain (Figure 4.6). In contrast to the behavior of the labrum in the larger tear group, the effect of increased biceps tension on the increased von Mises strain is relatively small in the smaller tear group (the models having no tear or a small SLAP tear). The surface strain in the smaller tear group was greater than the volume strain (Figure 4.6).

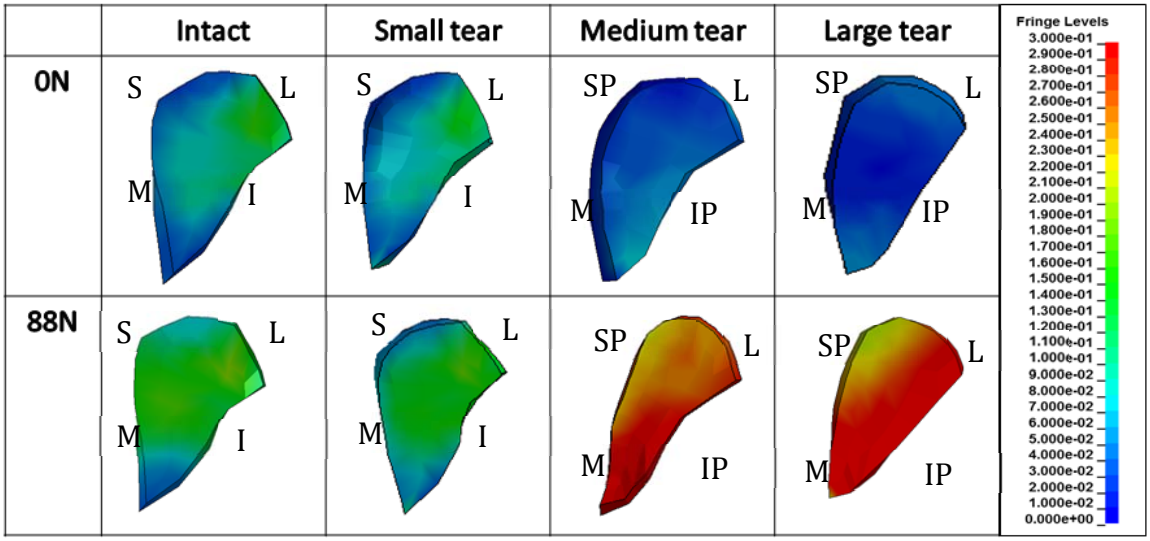

Figure 4.5 – The predicted von-Mises strain distribution at the cross section of the posterior edge for the SLAP tear and 0° for the intact labrum under 0 N and 88 N of biceps tension. S, M, I, L, SP, IP stand for superior, medial, inferior, lateral, supraposterior, inferoposterior, respectively.

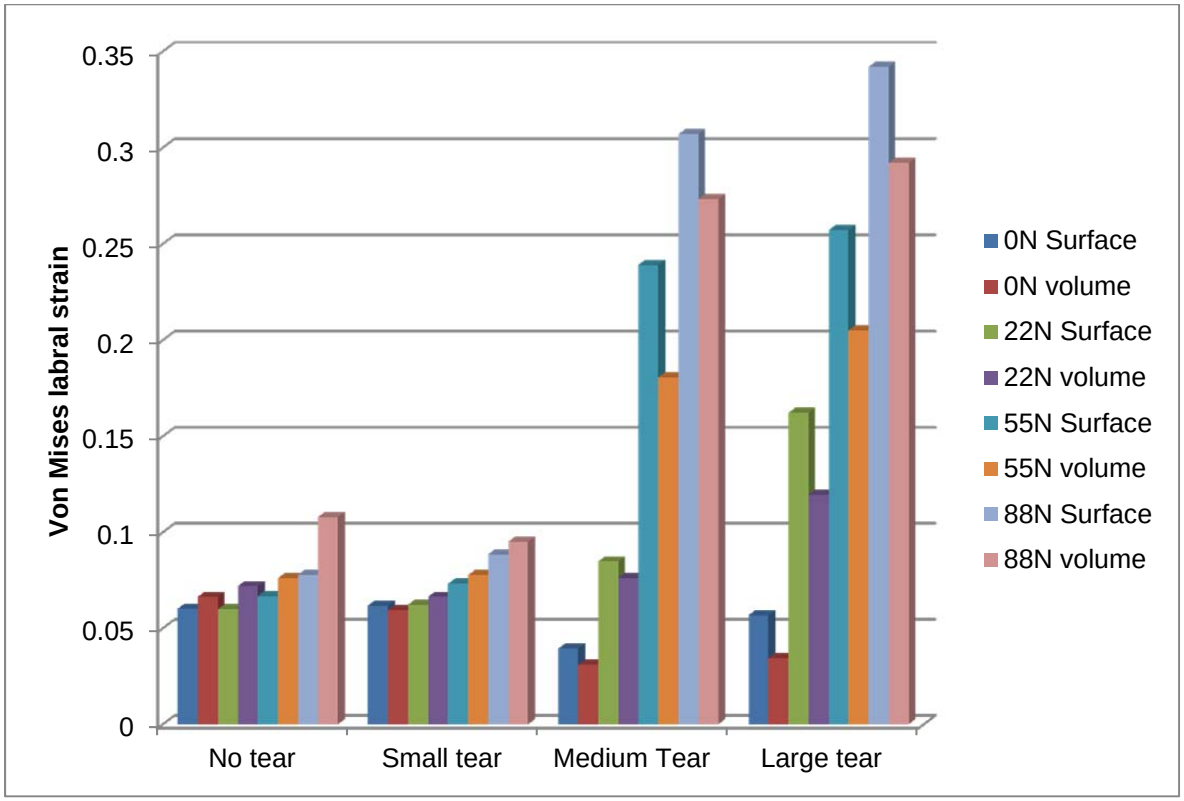

Figure 4.6 – The averaged von-Mises strain at the cross section of the posterior edge for the SLAP tear and the 0° location for the intact labrum.

Discussion

The purpose of this study was to understand the impact of the biceps on the propagation of the SLAP tear by observing the mechanical behavior of the torn superior glenoid labrum. The area of high strain in the torn labrum was found at the edge of each given tear (Figure 4.3). The strain on the labrum was increased with increased biceps tension regardless of the tear size but these correlations were stronger in the labrum having a medium or a large SLAP tear (Figure 4.4, Figure 4.5, and Figure 4.6). Therefore, this study supports the hypothesis that the SLAP tear might propagate as a result of the increasing tension on the long head of the biceps tendon.

The current study suggests that tension on the biceps attachment is a risk factor for propagation of a SLAP tear as well as for initiation of the SLAP tear. Based on mechanical testing,[41] traction on the biceps tendon can reproducibly create type II SLAP lesions. Our previous research[42] also demonstrates that the biceps tension plays a role in increased risk for SLAP tears. The biceps tension also shifted the location of the peak displacement from anterior to posterior attachment of the biceps tendon on the superior labrum. In this study, increasing tensile force of the biceps tendon resulted in increased strain of the intact labrum (Figure 4.4 and Figure 4.6). Moreover, the effect of biceps tension on the labral strain was emphasized in the torn labrum (Figure 4.4). With greater biceps tension, the peak of the maximum-principal strain at the edge of the given tear was also enlarged (Figure 4.3). Since the local strain adjacent to a tear has been accepted as an indicator of risk of tear propagation,[38] results suggest that increasing biceps tension increases the risk of tear progression.

Interestingly, the mechanical behavior of the torn labrum with a small detachment area was similar to that of the intact labrum except for a small risk for propagating the tear. The area

of high strain in the small tear model was predicted at the edge of the specific tear (Figure 4.3), and the magnitude of the maximum-principal strain at the area was slightly larger than that in the intact model (Figure 4.4). However, the predicted strains from the two models are significantly correlated. In addition to the peak strains, the strain distribution in the cross sectional area in the small tear model was also analogous to that in the intact model (Figure 4.5). This similarity could be explained by the mechanism of transferring and dissipating the biceps tension through the labrum in both radial and circumferential direction.[42] Using the intact model, a loading pathway in radial and circumferential directions was demonstrated. Since the majority of the labral tissues in the small tear model were connected to the glenoid rim, the radial and circumferential pathways are mostly intact. The higher volume-averaged strain among all elements in the cross section than the surface-averaged strain among elements on the interaction surface with the glenoid rim (Figure 4.6) suggest evidence of successful dissipation of the tensile force by the labrum tissue in the small tear model.

In contrast, the strain fields in the larger tear group present the effect of biceps tension on the strain distinctly with less dissipation of the tensile force. Without biceps tension, the labrum with a large tear is less deformed than the smaller tear group (Figure 4.4). This might be explained by its reduced constraints with increasing size of the tear. Increasing the biceps load causes a significant increase in the magnitude of the maximum-principal strain and the von-Mises strain (Figure 4.4 and Figure 4.6). This means that the risk of tear progression at the edge of the given tear is increased and the labrum experiences strains close to the failure strain. The reported failure strain for isolated labrum from human cadaver shoulders is approximately 40%.[43] Moreover, the surface-averaged strain is a greater than the volume-averaged strain (Figure 4.6). Therefore, the labrum tissues at the interaction surface with the glenoid rim are

more deformed than most of tissues in that cross section including the free edge surface. With increasing the distance between the posterior edge of the SLAP tear and the biceps anchor in a large tear model, the magnitude of strain at the lateral side is reduced. Based on these findings, it is proposed that the labrum with a large tear compromised in its ability to dissipate force in both radial and circumferential directions.

This study suggests that tear size should be a criteria for determining optimal treatment of the biceps tendon following SLAP tear. To date, age and physical activity were the general criteria for determining the optimal treatment.[18,19,20,21] However, this study shows that when other factors are equal, tear size determines the sensitivity of the labral strain to the biceps tension (Figure 4.4, Figure 4.5, and Figure 4.6). Thus, the tear size could be important factor to determine whether cutting the biceps tendon is recommended. When the labrum detachment involves only a small area, suturing the superior labrum to the glenoid rim could reduce the risk of tear progression. However, if the SLAP tear size is larger enough to be classified into the larger tear group in this study, then the biceps tenotomy could be the optimal treatment. This result corresponds well with clinical findings. According to Boileau and colleagues, cutting biceps can be considered an effective alternative to the repair of the SLAP tear[43]. Moreover, the long head of the biceps tendon is known as a pain generator in the setting of SLAP tear and cutting the tendon was recommended as the proper treatment by many clinical reports.[44,45] Since the repair of the SLAP tear after biceps tenotomy has been reported to make no difference of the glenohumeral kinematics,[31, 43] repair of the SLAP tear may not be required.

The current study was based on the predicted strain using a subject-specific finite element model, so this study also has the typical limitations. For this study, the geometry was acquired from one cadaver shoulder. Since the ability to apply this analysis is affected by how

representative this subject is to the general population, consideration of the anatomical variation is the necessary step. The glenoid labrum also has wide anatomical variations,[25,46,47,48] so the dimension of the specimen for this study was compared with that reported in the literatures.[22] The anterosuperior labrum has smaller volume in the specimen than both the volume of posterosuperior labrum in the same specimen and the volume of the anterosuperior labrum reported in the literature.[8,22,25] Thus, the force passing through the anterosuperior labrum tissue likely resulted in overestimated strains in the specific portion. Moreover, a finite element model requires material properties of each component. However, a huge variation on the mechanical properties of tissue has been reported depending on the measurement protocol or the process of the sample preparation.[25,27,46,47] To reduce the effect of this assumption on the results, the material sensitivity test was performed.[22] . Although the magnitude of the strain could be reduced by changes in the constitutive model for the labrum from the hyperelastic to the elastic model,[22] the robustness of the finite element model for predicting the distribution of the labral strain was demonstrated.[22] Thus, the role of biceps tension on the progression of SLAP tears based on the current study are not likely to be affected by this assumption.

In summary, the tension on the long head of the biceps tendon was more significant to tear propagation than to tear initiation on the superior glenoid labrum. The edge of the given tear on the labrum is suggested as the region into which the tear is most likely to propagate. Based on this study, the tear size should be added as a criteria in selecting the optimal treatment. The study supports the use of the biceps tenotomy in reducing the risk of progression of massive type II SLAP tears.

References

1. Snyder, S.J., Karzel, R.P., Pizzo, W.D., Ferkel, R.D., Friedman, M.J., 1990. SLAP lesions of the shoulder. Arthroscopy 6, 274-279.

2. Nam, E.K., Snyder, S.J., 2003. The diagnosis and treatment of superior labrum, anterior and posterior (SLAP) lesions. American Journal of Sports Medicine 31, 798-810.

3. Snyder, S.J., Banas, M.P., Karzel, R.P., 1995. An analysis of 140 injuries to the superior glenoid labrum. Journal of Shoulder and Elbow Surgery 4, 243-248.

4. Maffet, M.W., Gartsman, G.M., Moseley, B., 1995. Superior labrum-biceps tendon complex lesions of the shoulder. American Journal of Sports Medicine 23, 93-98.

5. Morgan, C.D., Burkhart, S.S., Palmeri, M., Gillespie, M., 1998. Type II SLAP lesions: three subtypes and their relationships to superior instability and rotator cuff tears. Arthroscopy 14, 553-565.

6. Kim,T.K., Queale, W.S., Cosgarea, A.J., McFarland, E.G., 2003. Clinical features of the different types of SLAP lesions: an analysis of one hundred and thirty-nine cases. Journal of Bone and Joint Surgery (American) 85-A:66-71.

7. Werner, C.M.L., Nyffeler, R.W., Jacob, H.A.C., Gerber, C., 2004. The effect of capsular tightening on humeral head translations. Journal of Orthopaedic Research 22, 194-201.

8. Smith, C.D., Masouros, S.D., Hill, A.M., Wallace, A.L., Amis, A.A., Bull, A.M., 2009. The compressive behavior of the human glenoid labrum may explain the common patterns of SLAP lesions. Arthroscopy 25, 504-509.

9. Andrews, J.R., Carson, W.G., Mcleod, W.D., 1985. Glenoid labrum tears related to the long head of the biceps. American Journal of Sports Medicine 13, 337-341.

10. Grauer, J.D., Paulos, L.E., Smutz, W.P., 1992. Biceps tendon and superior labral injuries. Arthroscopy 8, 488-497.

11. Jobe, C.M., 1995. Posterior superior glenoid impingement: expanded spectrum. Arthroscopy 11, 530-536.

12. Burkhart, S.S., Morgan, C.D., 1998. The peel-back mechanism: its role in producing and extending posterior type II SLAP lesions and its effect on SLAP repair rehabilitation. Arthroscopy 14, 637-640.

13. Pradhan, R.L., Itoi, E., Hatakeyama, Y, Urayama, M., Sato, K., 2001. Superior labral strain during the throwing motion: a cadaveric study. American Journal of Sports Medicine 29, 488-492.

14. Rizio, L., Garcia, J., Renard, R., Got, C., 2007. Anterior instability increases superior labral strain in the late cocking phase of throwing. Orthopedics 30, 544-550.

15. Kuhn, J.E., Lindholm, S.R., Huston, L.J., Soslowsky, L.J., Blasier, R.B., 2003. Failure of the biceps superior labral complex: a cadaveric biomechanical investigation comparing the late cocking and early deceleration positions of throwing. Arthroscopy 19, 373-379.

16. Yeh, M.L., Lintner, D., Luo, Z.P., 2005. Stress distribution in the superior labrum during throwing motion. American Journal of Sports Medicine 33, 395-401.

17. Costa Ado, S., Leite, J.A., Melo, F.E., Guimaraes, S.B., 2006. Biomechanical properties of the biceps-labral complex submitted to mechanical stress. Acta Cirurgica Brasileira 21, 214-218.

18. Boileau, P., Parratte, S., Chuinard, C., Roussanne, Y., Shia, D., Bicknell, R., 2009. Arthroscopic treatment of type II SLAP lesions: biceps tenodesis as an alternative to reinsertion. American Journal of Sports Medicine 37, 929-936.

19. Franceschi, F., Longo, U.G., Ruzzini, L., Rizzello, G., Maffulli, N., Denaro, V., 2008. No advantages in repairing a type II superior labrum anterior and posterior (SLAP) lesion when associated with rotator cuff repair in patients over age 50: a randomized controlled trial. American Journal of Sports Medicine 36, 247-253.

20. Neri, B.R., Vollmer, E.A., Kvitne, R.S., 2009. Isolated type II superior labral anterior posterior lesions: age-related outcome of arthroscopic fixation. American Journal of Sports Medicine 37m 937-942.

21. Zhang, A.L., Kreulen, C., Ngo, S.S., Hame, S.L., Wang, J.C., Gamradt, S.C., 2012. Demographic trends in arthroscopic SLAP repair in the united states. American Journal of Sports Medicine 40, 1144-1147.

22. Hwang, E.J., Carpenter, J., Hughes, R., Palmer, M.L., 2014. Shoulder labral pathomechanics with rotator cuff tears. Accepted. Journal of Biomechanics.

23. Anglin, C., Tolhurst, P., Wyss, U.P., Pichora, D.R., 1999. Glenoid cancellous bone strength and modulus. Journal of Biomechanics 32, 1091-1097.

24. Clavert, P., Zerah, M., Krier, J.,Mille, P., Kempf, J.F., Kahn, J.L., 2006. Finite element analysis of the strain distribution in the humeral head tubercles during abduction: comparison of young and osteoporotic bone. Surgical and Radiologic Anatomy 28, 581-587.

25. Carey, J., Small, C.F., Pichora, D.R., 2000. In situ compressive properties of the glenoid labrum. Journal of Biomedical Materials Research 51, 711-716.

26. Donzelli, P.S., Spilker, R.L., Ateshian, G.A., Mow, V.C., 1999. Contact analysis of biphasic transversely isotropic cartilage layers and correlations with tissue failure. Journal of Biomechanics 32, 1037-1047.

27. Smith, C.D., Masouros, S.D., Hill, A.M., Wallace, A.L., Amis, A.A., Bull, A.M., 2008. Tensile properties of the human glenoid labrum. Journal of Anatomy 212, 49-54.

28. Carpenter, J.E., Wening, J.D., Mell, A.G., Langenderfer, J.E., Kuhn, J.E., Hughes, R.E., 2005. Changes in the long head of the biceps tendon in rotator cuff tear shoulders. Clinical Biomechanics 20, 162-165.

29. Henak, C.R., Ellis, B.J., Harris, M.D., Anderson, A.E., Peters, C.L., Weiss, J.A., 2011. Role of the acetabular labrum in load support across the hip joint. Journal of Biomechanics 44, 2201-2206.

30. McMahon, P.J., Burkhart, A., Musahl, V., Debski, R.E., 2004. Glenohumeral translations are increased after a type II superior labrum anterior-posterior lesion: a cadaveric study of severity of passive stabilizer injury. Journal of Shoulder and Elbow Surgery 13, 39-44.

31. Patzer, T., Habermeyer, P., Hurschler, C., Bobrowitsch, E., Wellmann, M., Kircher, J., Schofer, M.D., 2010. The influence of superior labrum anterior to posterior (SLAP) repair on restoring baseline glenohumeral translation and increased biceps loading after simulated SLAP tear and the effectiveness of SLAP repair after long head of biceps tenotomy. Journal of Shoulder and Elbow Surgery 21, 1580-1587.

32. Gatti, C.J., Maratt, J.D., Palmer, M.L., Hughes, R.E., Carpenter, J.E., 2010. Development and validation of a finite element model of the superior glenoid labrum. Annals of Biomedical Engineering 38, 3766-3776.

33. Youm, T., ElAttrache, N.S., Tibone, J.E., McGarry, M.H., Lee, T.Q., 2009. The effect of the long head of the biceps on glenohumeral kinematics. Journal of Shoulder and Elbow Surgery 18, 122-129.

34. Su, W.R., Budoff, J.E., Luo, Z.P., 2010. The effect of posterosuperior rotator cuff tears and biceps loading on glenohumeral translation. Arthroscopy 26, 578-586.

35. Langenderfer, J., LaScalza, S., Mell, A., Capenter, J.E., Kuhn, J.E., Hughes, R.E., 2005. An EMG-driven model of the upper extremity and estimation of long head biceps force. Computers in Biolology and Medicine 35, 25-39.

36. McCully, K.K., Faulkner, J.A., 1985. Injury to skeletal muscle fibers of mice following lengthening contractions. Journal of Applied Physiology 59, 119-126.

37. Drury, N.J., Ellis, B.J., Weiss, J.A., McMahon, P.J., Debski, R.E., 2010. The impact of glenoid labrum thickness and modulus on labrum and glenohumeral capsule function. Journal of Biomechanical Engineering 132, 121003.

38. Andarawis-Puri, N., Ricchetti, E.T., Soslowsky, L.J., 2009. Rotator cuff tendon strain correlates with tear propagation. Journal of Bioemechanics 42, 158-163.

39. Drury, M.J., Ellis, B.J., Weiss, J.A., McMahon, P.J., Debski, R.E., 2011. Finding consistent strain distributions in the glenohumeral capsule between two subjects: implications for development of physical examinations. Journal of Biomechanics 44, 607-613.

40. Yeh, M.L., Lintner, D., Luo, Z.P., 2005. Stress distribution in the superior labrum during throwing motion. American Journal of Sports Medicine 33, 395-401.

41. Bey, M.J., Elders, G.J., Huston, L.J., Kuhn, J.E., Blasier, R.B., Soslowsky, L.J., 1998. The mechanism of creation of superior labrum, anterior, and posterior lesions in a dynamic biomechanical model of the shoulder: the role of inferior subluxation. Journal of Shoulder and Elbow Surgery 7, 397-401.

42. Hwang, E.J., Carpenter, J., Hughes, R., Palmer, M.L., 2013. Effects of biceps tension and superior humeral head translation on the glenoid labrum. In review. Journal of Orthopaedic Research.

43. Boileau, P., Parratte, S., Chuinard, C., Roussanne, Y., Shia, D., Bicknell, R., 2009. Arthroscopic treatment of isolated type II SLAP lesions: Biceps tenodesis as an alternative to reinsertion. American Journal of Sports Medicine 37; 929-936.

44. Provencher, M.T., McCormick, F., Dewing, C., McIntire, S., Solomon, D., 2013. A prospective analysis of 179 type 2 superior labrum anterior and posterior repairs: outcomes and factors associated with success and failure. American Journal of Sports Medicine 41, 880-886.

45. Walch,G., Edwards, T.B., Boulahia, A., Nove-Josserand, L., Neyton, L., Szabo, I., 2005. Arthroscopic tenotomy of the long head of the biceps in the treatment of rotator cuff tears: clinical and radiographic results of 307 cases. Journal of Shoulder and Elbow Surgery 14, 238-246.

46. Vangsness, C.T., Jr., Jorgenson, S.S., Watson, T., Johnson, D.L., 1994. The origin of the long head of the biceps from the scapula and glenoid labrum. An anatomical study of 100 shoulders. Journal of Bone and Joint Surgery (British) 76, 951-954.

47. Tuoheti, Y., Itoi, E., Minagawa, H., Yamamoto, N., Saito, H., Seki, N., Okada, K., Shimada, Y., Abe, H., 2005. Attachment types of the long head of the biceps tendon to the glenoid labrum and their relationships with the glenohumeral ligaments. Arthroscopy 21, 1242-1249.

48. Huang, C.Y., Stankiewicz, A., Ateshian, G.A., Mow, V.C., 2005. Anisotropy, inhomogeneity, and tension-compression nonlinearity of human glenohumeral cartilage in finite deformation. Journal of Biomechanics 38, 799-809.

CHAPTER V

GENERAL DISCUSSION

Innovation

This is the first study to address the effects of tension on the long head of the biceps tendon and superior translation of the humeral head on both the initiation and propagation of SLAP tears using finite element model. Based on predicted strain (Chapter II), the significant role of the superior humeral head translation in the initiation (Chapter III) and the biceps tension in the propagation of SLAP tears (Chapter IV) was observed.

The extended and validated finite element model[1] (Chapter II) is the first model to include loading of the long head of the biceps tendon for the study of the mechanism of SLAP tears. Although both tension on the biceps tendon and humeral head translation were known as factors influencing SLAP tear pathology, no histologic[2,3,4], arthroscopic[2,4,5,6,7], and biomechanical studies,[8,9,10,11,12,13,14,15,16,17,18] could explain the relative contribution of those factors in the genesis and/or progression of SLAP tears. Unlike cadaveric experiments or clinical studies, this study using a finite element model allows an unlimited number of testing without fatigue or damage of the tissues, systematically controlling for finding the cause-effect relationships between parameters, and observation of mechanics inside of tissue. The ability to

cover the large variation in material properties is another general benefit of finite element model, so the results form a well-developed model with many advantages that complement other study designs. Few finite element models have been developed to understand the behavior of the labrum. Yeh and his colleagues[19] studied the stress concentration at the glenoid bone using a simplified non-anatomic axisymmetric finite element model including the glenoid bone, the labrum, and the anchor of the biceps tendon on the superior labrum. Drury et al.[20] analyzed the strain distribution at the medial portion of the capsule using the finite element model, including the humerus, scapula and capsule regions with a two-dimensional model of the labrum. The finite element model, developed by Gatti et al.[21] was the only model having an anatomically accurate labrum. Gatti's model included the humeral head cartilage, glenoid cartilage, and labrum. Due to the absence of the biceps tendon in all previous models, none of them were able to test mechanical hypotheses relevant to the biceps tension as well as humeral head motion. The model for the current study consisted of anatomically accurate components of following: humerus, glenoid bone, humeral head cartilage, glenoid cartilage, labrum, and biceps tendon. This model predicted the strain pattern within the labrum tissue caused from both biceps tension and humeral head translation. Since high strain is considered an indicator of the risk for the pathology,[22,23] this finite element model[23] is the first model to explain the impacts of both factors on the SLAP tear pathology.

This is the first investigation on the mechanism of both the genesis (Chapter III) and progression (Chapter IV) of the SLAP tear with consideration of two factors: namely loading on the biceps tendon and migration of the humeral head. Similar to the tear on the superior labrum, the supraspinatus tendon, which is usually the first tendon of the rotator cuff to be injured, also experiences lesions at its insertion to the humeral greater tuberosity. For this tear, both the

initiation[24,25,26], and propagation of the supraspinatus tendon tear[22,27,28] have been actively studied. Contrary to studies on the supraspinatus tendon tear, the labral tear studies concentrated on the mechanism of initiation and none of the previous studies of the SLAP tear addressed the progression of the tear. The current study is the first to examine the strain distribution in the torn labrum as well as the intact labrum tissue. Therefore, this work is the first modeling investigation of the progression of the SLAP tear.

Significance

There remains controversy over the role of the biceps tendon in the SLAP tear, and thereby on the best management of a tear involving biceps tendon, which is the most common SLAP tear. Using a well-validated finite element model (Chapter II), one can better understand the mechanism of initiation (Chapter III) and propagation (Chapter IV) of the SLAP tear. By identifying factors that may contribute to the initiation and propagation of tears, the current study suggests a criterion to improve treatment approaches.

Discrepancy in the role of the biceps tendon in the labrum tear

Surgeons and researchers had been faced with contradictory evidence regarding the function of the long head of the biceps tendon in the initiation of the labrum tear. The genesis of SLAP tears in multiple pitching phases or with pulling of the biceps tendon was observed, but researchers arrived at two different debatable findings in each issue. However, the current study can explain the knowledge gap created by conflicting reports.

There is disagreement as to the effect of the biceps tension on the initiation of SLAP tear. With examination of the presence of a SLAP tear after pulling of the biceps tendon, two opposite observations were reported.[11,12] Bey and his colleagues[11] applied a tensile force to the long head of the biceps tendon in anatomic axis (overall, lateral direction). They found the biceps tension is capable of generating a SLAP lesion in some reduced and most inferiorly subluxed glenohumeral positions. On the contrary, Costa et al.[12] applied the traction of the biceps tendon in superior direction, an unusual force vector for the biceps muscle, until the distal portion of the tendon was ruptured. With observation of no SLAP tear, Costa et al. argued that either simple continuous or a sudden uniaxial traction of the biceps tendon do not affect the genesis of a SLAP lesion. The

current work directly provided the important role of biceps tension in the initiation of a tear (Chapter III) by loading the biceps tension along the force vector of the biceps muscle. Furthermore, the impact of biceps tension is more critical on the torn labrum (Chapter IV) than the intact labrum. Thus, from this study and considering the force vector of the biceps muscle, the two opposing opinions can be reconciled. The biceps tension plays a considerable role in the initiation of the SLAP tear and a substantial role in the propagation of an existing SLAP tear.

Disagreement on the optimal treatment for the most common SLAP tear

There are debates among surgeons on the optimal treatment and the results of the treatment for the biceps tendon following a SLAP tear. However, the current study (Chapter IV) suggests a criterion, tear size at the time of the surgery, for selection of the best treatment to decrease the risk of progression of a SLAP tear. Furthermore, with additional studies on other related clinical problems using the finite element model for a SLAP tear (Chapter II), proper treatments to reduce the rate of SLAP tear recurrence might be proposed leading to the selection of specific surgical procedures to minimize the effect on glenohumeral kinematics.

Surgeons continue to debate the best treatment to reduce a pain for patients among arthroscopic repair, debridement, tenodesis, tenotomy, or solely observation,[29,30,31,32,33] but the reported outcomes of repair SLAP lesion are also variable.[34,35,36] When considering the rate of returning to previous level of activity after repair of SLAP tears, the outcomes ranges from 20% to 84%.[5,36,37,38] This large range suggests there might be unaccounted for factors in the SLAP tear mechanism. Until now, the known criteria to determine the optimal treatment of type II SLAP tear were age and physical activity.[29,39] However, this work supports adding one criteria, the current size of tear (Chapter IV), to determine treatment of the SLAP tear. Suturing superior

labrum to the glenoid rim is advisable treatment to the shoulder having a small SLAP tear, whereas biceps tenotomy maybe recommended for patients having a large SLAP tear (Chapter IV). Cutting the biceps tendon in patients with a large labral tear is advocated by the clinical literature.[40,41,42,43,44]

In addition, there is a discrepancy concerning the effectiveness of treatment of the type II SLAP lesion on restoring stability or kinematics of the glenohumeral joint. Cadaveric studies have reported the arthroscopic SLAP repair of the experimental SLAP lesion could recover nearly normal biomechanics, but biceps tenotomy could not.[14,37,44,45,46,47,48,49,50,51] Thus, cadaveric studies suggest an arthroscopic SLAP repair for recovering glenohumeral stability. On the contrary, clinical studies have found no clinically demonstrable alteration in kinematics after biceps tenotomy or tenodesis and more favorable outcomes with cutting biceps tendon.[29,39,44,51] Therefore, clinical studies recommend cutting the biceps tendon to restore glenohumeral kinematics. These controversial findings arise from contradictions surrounding the biomechanical function of the biceps tendon. One possible explanation is the long head of the biceps co-operates with other muscles in the stability of the glenohumeral joint in *in vivo*. The related kinematic changes, resulting from cutting the biceps tendon with and without increased forces of other musculatures in the glenohumeral joint, could be studied by extending the current finite element model (Chapter II). Moreover, the multiple re-fixation techniques[13,14,34] of the SLAP lesion, which vary in type, position, number of fixation devices, and method of securing the labrum,[51] could be efficiently evaluated using an extended model from the finite model in this work.

Limitations

This study used the finite element model, so limitations of the current work include those inherent in a finite element model of simulated injuries to the tissues in the human body. Acquisition of geometrical information and defining the material properties were the most challenging steps in development of a finite element model for soft tissues. The multiple dynamic reactions or healing potential that are present *in vivo* were not included in this model. For understanding of the tear propagation, introducing a SLAP lesion on the labrum, produced by detaching a surface of the labrum from the glenoid rim, probably over-simplify the complex clinical and histological presentation of the tear. In addition, findings in this study is a labrum centric interpretation.

Variation in information for finite element model

The finite element model was generated with geometrical information acquired from one specimen, and material information averaged from other specimens. Moreover, high variation has been reported in both anatomy[2,3,4,7,8,9,10] and material properties[8,9,10] of the labrum. Thus, the effect of these variations on the prediction by the finite element model should be considered in the analysis of results.

This study developed a subject-specific three-dimensional finite element model and compared the anatomy of the tissue for the model to published general anatomy in order to reduce the effect of anatomical variances of the factors considered in the analysis. Anatomical variations on the labrum and the attachment of the biceps tendon on the superior labrum has been reported.[2,7,9,10,20] The significant differences in the predicted stress and strain have also been represented with variation in the anatomy of the tissue.[19,20,52] In hip labrum model, simplification

to the geometry generated about 50% of difference in the prediction.[53] In the glenoid labrum model, the magnitude of strain in the capsule differed about 30% [20] and that in the glenoid bone differed about 30% [19] with simplification of the labral anatomy. However, due to difficulty of finding the boundary between the glenoid labrum and other connective soft tissues,[20,21] the early models of the labrum were either simplified axisymmetric model[19] (Figure 5.1) or simplified two-dimensional model (Figure 5.2)[20]. Moreover, those omitted important components on the transferring of the stress during the simulation, and did not validate finite element predictions of the strain. Gatti et al. generated a three-dimensional finite element model (Figure 5.3)[21] from a specific subject, but it does not include the biceps tendon. This model also used tetrahedral meshes, yet hexahedral meshes are more popular in biomechanical field [53,54,55] due to improved robustness and better representation of the material characteristics.[21,56,57] However, this work is the first and only attempt to develop a three-dimensional hexahedral model, using subject-specific geometry, for the SLAP tear pathology. In addition, the current thesis was based on the finite element model from just one specimen. Thus, this study also compared the anatomic characteristics of the specimen for the model with the published anatomical information averaged from more samples,[8,9] as well as comparison of the anatomy within the labrum tissue of the specific subject for the finite element model. The effect of difference in the anatomical information on the predicted strain pattern was discussed in each chapter.

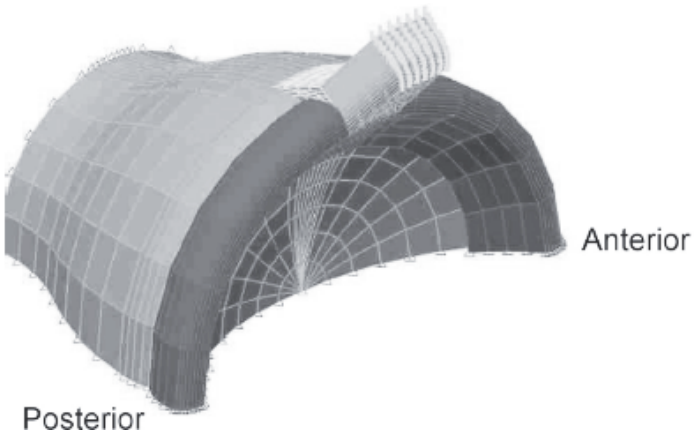

Figure 5.1 - The axisymmetric finite element model of the superior glenoid labrum for the simulation of throwing motion[19]

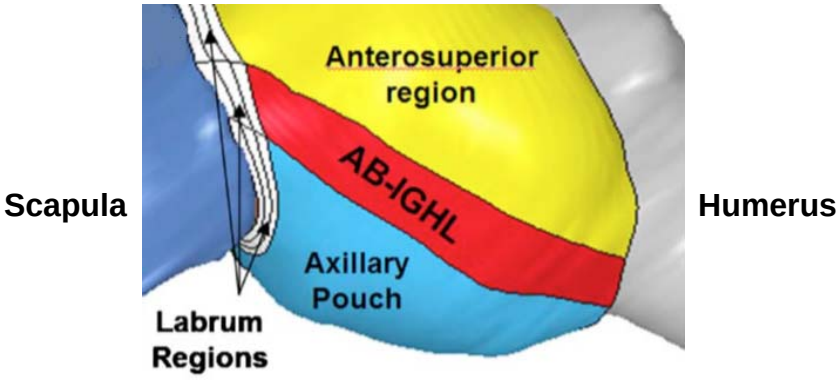

Figure 5.2 - The two-dimensional finite element model having the labrum, introduced in the glenohumeral joint model in white by simply redefining the medial side of capsule elements as the labrum.[20.] This model is in the coronal view from an inferior perspective.

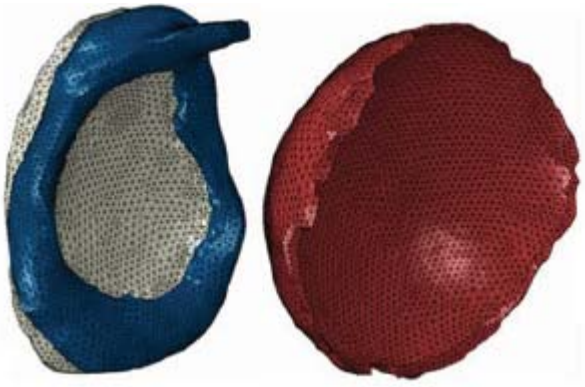

Figure 5.3 - The subject-specific tetrahedral finite element model of the glenoid labrum in lateral view.[21]

The current finite element model tested the sensitivity of the predictions to material properties by varying both the constitutive representation and the material properties. Significant change in the results with changing both material properties and constitutive representation[52,57,58,59,60] and a wide range of properties for tissues in the finite element model in the literature[9,10,58,65,66,67] have been reported. The previous simplified finite element models[19,20] also simplified and equalized the material behavior of the labrum to that of the neighboring tissues, such as the biceps tendon[19] or capsule.[20] Therefore, the labrum for those studies was defined using a linear, isotropic constitutive law having a difference of at least one order of magnitude from the published properties for the labrum tissue.[8,10] However, the current finite element model used the latest published data for assigning material properties for each tissue (Table 2.1 in Chapter II). Clearly, the latest reported material properties[8,9] could not directly reflect the detailed microstructural characteristics,[2,3,7,54,64,65] because of both technical limitation of the cadaveric biomechanical experiments and complex interfaces between the labrum and connective tissues. Nevertheless, results from the material sensitivities test for the current finite element model (Chapter II) represented the material properties may impact the magnitude of the strain, but not to the general strain distribution.[22,25]

Simplifying information for finite element model

The current finite element model relies on the simplification of dynamic clinical behavior of tissues, such as biceps tendon, rotator cuff, even torn labrum. In the clinical scenario, the problematic tissue might naturally heal with time or the reduced function caused from the problem could be compensated by adaption or remodeling of other surrounding structures.

While adaptive mechanisms have been studied using finite element model,[66,67,68] these processes were not represented in this study.

First, the behavior of the biceps tendon is simplified. The amount of biceps tension was determined based on physiological cross sectional areas and reported in the literature. The physiological cross sectional area of the long head of the biceps has been reported as 2.5 ± 0.5 cm^2 or 2.5 ± 1.1 cm^2 at the elbow joint[69, 70] and 2.11 ± 2.0 cm^2 at the shoulder joint[71] using following formula: muscle volume/fiber length[72] or muscle volume/ fiber length·cosϕ[73]. The muscle force can be computed by physiological cross sectional area·specific tension·cosϕ[74], or physiological cross sectional area·specific tension[73]. Using either of these definitions[73,74], or a conversion factor of 3.5kg/cm^2 for potential maximum force,[48,75] the physiological maximum lengthening force generated by the long head of the biceps muscle is similar to 88N, which is used in other studies.[76] With age-related reduction of cross sectional area,[77, 78, 79] the maximum force may be reduced in the elderly. However, this is all based on the assumption that the specific tensions across subjects are the same.

Second, the rotator cuff tear was simulated by humeral head translation in superior direction. With rotator cuff tears, the concavity and compressive force of the glenohumeral joint is reduced. The combination of this reduction and the unchanged deltoid muscle force in superior direction may result in migration of the humeral head in superior direction. In the clinical studies,[80, 81, 82] superior translation of the humeral head is a common occurrence in patients having large rotator cuff tear. In clinical studies, the maximum amount of translation has been reported up to 5mm. Thus, the humeral head was translated up to that amount in the simulation.

Thirdly, the behavior of the torn labrum could be overly-simplified. In reality, fraying of the outer edge of the superior labrum with type II SLAP tear might be found.[83,84] However, in the

model, the SLAP tear was introduced by detaching a surface of the superior labrum from the corresponding glenoid rim. There are two reasons. One is that the area of high strain was found at the mid-substance of the interface between the superior labrum and glenoid rim[1,23] not the possible area for fraying. The other is that sharply cutting the labrum from its attachment to the glenoid was generally used and accepted for creation of a SLAP lesion in cadaveric studies.[13,14,37,44,45,85]

Future Directions

Multiple hypotheses and questions could be tested and answered with extension of the finite element model for this work. The effect of the arm position with biceps loading and the effect of biceps tenotomy on the mechanism of the SLAP tear are good examples.

The change in the arm position, especially with axial rotation, could change the loading vector and morphology of the biceps tendon, thus may have an impact on the SLAP tear mechanism. The increasing external rotation accompanied by increasing biceps tension has been reported to significantly increase the surface strain of the labrum.[15,16,86] External or internal rotation in the humerus axis alters the primary loading vector of the long head of the biceps tendon either in the posterior or the inferior direction. This change in the force vector of the biceps tendon could influence the strain distribution. For example, cadaveric study reported that the late cocking phase of the pitching motion, when the arm is placed in maximally external rotation and maximally tensed, generated greater strain in the superoposterior labrum than strain in the superoinferior labrum.[15] Moreover, there is a chance for the biceps tendon to be twisted with the arm rotation in humerus axis similar to the behavior of the supraspinatus tendon.[87] In this case, the anchor of the biceps tendon on the superior labrum could be twisted and pulled out, so that a greater concentration of the load at the anchor attachment could be expected. This may increase the risk of the SLAP tear. In other words, the arm posture could be the factor to affect both initiation and propagation of the SLAP tear. Therefore, investigating the effect of arm position on the SLAP tear mechanism by extending of the current finite element model having both intact and torn labrum in it could be a critical study for understanding the SLAP tear.

The benefit of the SLAP repair after the biceps tenotomy could be evaluated by modifying the current finite element model. With biceps tenomoty, the tension on the biceps

tendon does not impact on the increasing the labral strain anymore. According to cadaveric studies,[37,45] the SLAP repair after cutting the biceps tendon has been reported to have no substantial impact on glenohumeral kinematics. However, at the same time, the burden of decreased stabilizing function by cutting the biceps tendon[37,46,47,88] could fall on the labrum. Under this scenario, the labrum after biceps tenotomy may experience greater stress during arm motion than the labrum before tenotomy. When considering of the tear propagation is highly correlated with the strain pattern caused by stress on the tissue,[22] the biceps tenotomy may accelerate the labral tear propagation. Thus, a study on the benefit of the SLAP repair following biceps tenotomy for the torn labrum could be important future study to improve treatment of SLAP tear.

The diverse surgical approaches could be simulated with the finite element model for this work and the results to the labrum tissue additionally predicted. The multiple re-fixing techniques for the torn superior labrum were simulated with the cadaveric shoulder. The glenohumeral kinematics[14] or the load to ultimate failure[13] was studied with most common suture techniques, such as using screw-in anchors,[13] using bio-absorbable tissue tacks,[13,14] and using a knotless anchor.[14] However, the extended finite element model from the current model could evaluate the effect of techniques on the labrum directly. This approach may allow general understanding on the suture techniques as well as pros and cons of each technique.

References

1. Hwang, E.J., Carpenter, J., Hughes, R., Palmer, M.L., 2014. Effects of biceps tension and superior humeral head translation on the glenoid labrum. In review of 1st revision. Journal of Orthopaedic Research.

2. Tuoheti, Y., Itoi, E., Minagawa, H., Yamamoto, N., Saito, H., Seki, N., Okada, K., Shimada, Y., Abe, H., 2005. Attachment types of the long head of the biceps tendon to the glenoid labrum and their relationships with the glenohumeral ligaments. Arthroscopy 21, 1242-1249.

3. Hill, A.M., Hoerning E.J., Brook, K., Smith, C.D., Moss, J., Ryder, T., Wallace, A.L., Bull, A.M.J., 2008. Collagenous microstructure of the glenoid labrum and biceps anchor. Journal of Anatomy 212, 853-862.

4. Pfahler, M., Haraida, S., Schulz, C., Anetzberger, H., Refior, H.J., Bauer, G.S., Bigliani, L.U., 2003. Age-related changes of the glenoid labrum in normal shoulders. Journal of Shoulder and Elbow Surgery 12, 40-52.

5. Kim, T.K., Queale, W.S., Cosgarea, A.J., McFarland, E.G., 2003. Clinical features of the different types of SLAP lesions: an analysis of one hundred and thirty-nine cases. Journal of Bone and Joint Surgery (American) 85-A, 66-71.

6. Snyder, S.J., Banas, M.P., Karzel, R.P., 1995. An analysis of 140 injuries to the superior glenoid labrum. Journal of Shoulder and Elbow Surgery 4, 243-248.

7. Vangsness, C.T., Jr., Jorgenson, S.S., Watson, T., Johnson, D.L., 1994. The origin of the long head of the biceps from the scapula and glenoid labrum. An anatomical study of 100 shoulders. Journal of Bone and Joint Surgery (British) 76, 951-954.

8. Smith, C.D., Masouros, S.D., Hill, A.M., Wallace, A.L., Amis, A.A., Bull, A.M., 2009. The compressive behavior of the human glenoid labrum may explain the common patterns of SLAP lesions. Arthroscopy 25, 504-509.

9. Carey, J., Small, C.F., Pichora, D.R., 2000. In situ compressive properties of the glenoid labrum. Journal of Biomedical Materials Research 51, 711-716.

10. Smith, C.D., Masouros, S.D., Hill, A.M., Wallace, A.L., Amis, A.A., Bull, A.M., 2008. Tensile properties of the human glenoid labrum. Journal of Anatomy 212, 49-54.

11. Costa Ado, S., Leite, J.A., Melo, F.E., Guimaraes, S.B., 2006. Biomechanical properties of the biceps-labral complex submitted to mechanical stress. Acta Cirurgica Brasileira 21, 214-218.

12. Bey, M.J., Elders, G.J., Huston, L.J., Kuhn, J.E., Blasier, R.B., Soslowsky, L.J., 1998. The mechanism of creation of superior labrum, anterior, and posterior lesions in a dynamic

biomechanical model of the shoulder: the role of inferior subluxation. Journal of Shoulder and Elbow Surgery 7, 397-401.

13. DiRaimondo, C.A., Alexander, J.W., Noble, P.C., Lowe, W.P., Lintner, D.M., 2004. A biomechanical comparison of repair techniques for type II SLAP lesions. American Journal of Sports Medicine 32, 727-733.

14. Uggen, C., Wei, A., Glousman, R.E., ElAttrache, N., Tibone, J.E., McGarry, M.H., Lee, T.Q., 2009. Biomechanical comparison of knotless anchor repair versus simple suture repair for type II SLAP lesions. Arthroscopy 25, 1085-1092.

15. Pradhan, R.L., Itoi, E., Hatakeyama, Y, Urayama, M., Sato, K., 2001. Superior labral strain during the throwing motion: a cadaveric study. American Journal of Sports Medicine 29, 488-492.

16. Rizio, L., Garcia, J., Renard, R., Got, C., 2007. Anterior instability increases superior labral strain in the late cocking phase of throwing. Orthopedics 30, 544-550.

17. Kuhn, J.E., Lindholm, S.R., Huston, L.J., Soslowsky, L.J., Blasier, R.B., 2003. Failure of the biceps superior labral complex: a cadaveric biomechanical investigation comparing the late cocking and early deceleration positions of throwing. Arthroscopy 19, 373-379.

18. Healey, J.H., Barton, S., Noble, P., Kohl, H.W., 3rd, Ilahi, O.A., 2001. Biomechanical evaluation of the origin of the long head of the biceps tendon. Arthroscopy 17, 378-382.

19. Yeh, M.L., Lintner, D., Luo, Z.P., 2005. Stress distribution in the superior labrum during throwing motion. American Journal of Sports Medicine 33, 395-401.

20. Drury, N.J., Ellis, B.J., Weiss, J.A., McMahon, P.J., Debski, R.E., 2010. The impact of glenoid labrum thickness and modulus on labrum and glenohumeral capsule function. Journal of Biomechanical Engineering 132, 121003.

21. Gatti, C.J., Maratt, J.D., Palmer, M.L., Hughes, R.E., Carpenter, J.E., 2010. Development and validation of a finite element model of the superior glenoid labrum. Annals of Biomedical Engineering 38, 3766-3776.

22. Andarawis-Puri, N., Ricchetti, E.T., Soslowsky, L.J., 2009. Rotator cuff tendon strain correlates with tear propagation. Journal of Bioemechanics 42, 158-163.

23. Hwang, E.J., Carpenter, J., Hughes, R., Palmer, M.L., 2014. Shoulder labral pathomechanics with rotator cuff tears. Accepted. Journal of Biomechanics.

24. Seki, N., Itoi, E., Shibuya, Y., Wakabayashi, I, Sano, H., Sashi, R., Minagawa, H., Yamamoto, N., Abe, H., Kikuchi, K., Okada, K., 2008. Mechanical environment of the supraspinatus tendon: three-dimensional finite element model analysis. Journal of Orthopaedic Science 13, 348-353.

25. Inoue, A., Chosa, E., Goto, K., Tajima, N., 2012. Nonlinear stress analysis of the supraspinatus tendon using three-dimensional finite element analysis. Knee Surgery, Sports Traumatology, Arthroscopy 21, 1151-1157.

26. Wakabayashi, I., Itoi, E., Sano, H., Shibuya, Y., Sashi, R., Minagawa, H., Kobayashi, M., 2003. Mechanical environment of the supraspinatus tendon: a two-dimensional finite element model analysis. Journal of Shoulder and Elbow Surgery 12, 612-617.

27. Reilly, P., Amis, A.A., Wallace, A.L., Emery, R.J.H., 2003. Supraspinatus tears: Propagation and strain alteration. Journal of Shoulder and Elbow Surgery 12, 134-138.

28. Sano, H., Wakabayashi, I., Itoi, E., 2006. Stress distribution in the supraspinatus tendon with partial-thickness tears: An analysis using two-dimensional finite element model. Journal of Shoulder and Elbow Surgery 15, 100-105.

29. Boileau, P., Parratte, S., Chuinard, C., Roussanne, Y., Shia, D., Bicknell, R., 2009. Arthroscopic treatment of type II SLAP lesions: biceps tenodesis as an alternative to reinsertion. American Journal of Sports Medicine 37, 929-936.

30. Franceschi, F., Longo, U.G., Ruzzini, L., Rizzello, G., Maffulli, N., Denaro, V., 2008. No advantages in repairing a type II superior labrum anterior and posterior (SLAP) lesion when associated with rotator cuff repair in patients over age 50: a randomized controlled trial. American Journal of Sports Medicine 36, 247-253.

31. Neri, B.R., Vollmer, E.A., Kvitne, R.S., 2009. Isolated type II superior labral anterior posterior lesions: age-related outcome of arthroscopic fixation. American Journal of Sports Medicine 37, 937-942.

32. Zhang, A.L., Kreulen, C., Ngo, S.S., Hame, S.L., Wang, J.C., Gamradt, S.C., 2012. Demographic trends in arthroscopic SLAP repair in the united states. American Journal of Sports Medicine 40, 1144-1147.
33. Hsu, A.R., Ghodadra, N.S., Provencher, C.M.T., Lewis, P.B., 2011. Biceps tenotomy versus tenodesis: a review of clinical outcomes and biomechanical results. Journal of Shoulder and Elbow Surgery 20, 326-332.

34. Osti, L., Soldati, F., Cheli, A., Pari, ., Massari, L., Maffulli, N., 2012. Biceps instability and slap type II tear in overhead athletes. Muscles, Ligaments and Tendons Journal 2, 258-266.

35. Brockmeier, S.F., Voos, J.E., Williams, R.J., Altchek, D.W., Cordasco, F.A., Allen, A.A., 2009. Outcomes after arthroscopic repair of type-II SLAP lesions. Journal of Bone and Joint Surgery (American). 91, 1595-1603.

36. Gorantla, K., Gill, C., Wright, R.W., 2010. The Outcome of Type II SLAP Repair: A Systematic Review. Arthroscopy 26, 537-545.

37. Strauss, E.J., Salata, M.J., Sershon, R.A., Garbis, M., Provencher, M.T., Wang, V.M., McGill, K.C., Bush-Joseph, C.A., Nicholololson, G.P., Cole, B.J., Romeo, A.A., Verma, N.N., 2013. Role of the superior labrum after biceps tenodesis in glenohumeral stability. Journal of Shoulder and Elbow Surgery, In press.

38. Ide, J., Maeda, S., Takagi, K., 2005. Sports activity after arthroscopic superior labral repair using suture anchors in overhead-throwing athletes. American Journal of Sports Medicine 33, 507-514.

39. Provencher, M.T., McCormick, F., Dewing, C., McIntire, S., Solomon, D., 2013. A prospective analysis of 179 type 2 superior labrum anterior and posterior repairs: outcomes and factors associated with success and failure. American Journal of Sports Medicine 41, 880-886.

40. Mariani, E.M., Cofield,R.H., Askew, L.J., Li, G., Chao, E.Y.S., 1988. Rupture of the tendon of the long head of the biceps brachii: Surgical versus nonsurgical treatment. Clinical Orthopaedics and Related Research 228, 233-239.

41. Neer CS II, 1990. Shoulder construction, Saunders, Philadelphia.

42. Sethi, N., Wright, R., Yamaguchi, K., 1999. Disorders of the long head of the biceps tendon. Journal of Shoulder and Elbow Surgery 8, 644-654.

43. Walch, G., Edwards, T.B., Boulahia, A., Nove-Josserand, L., Neyton, L., Szabo, I., 2005. Arthroscopic tenotomy of the long head of the biceps in the treatment of rotator cuff tears: clinical and radiographic results of 307 cases. Journal of Shoulder and Elbow Surgury 14, 238-246.

44. Alexander S, Southgate D, Hill A, Wallace A, Bull A. The role of the biceps tendon in passive translation of the glenohumeral joint. In.
SECEC/ ESSSE Annual Conference. Brugge, Belgium; 2008, O44.

45. Patzer, T., Habermeyer, P., Hurschler, C., Bobrowitsch, E., Wellmann, M., Kircher, J., Scholfer, M.D., 2011. The influence of superior labrum anterior to posterior (SLAP) repair on restoring baseline glenohumeral translation and increased biceps biceps loading after simulated SLAP tear and the effectiveness of SLAP repair after long head of biceps tenotomy. Journal of Shoulder and Elbow Surgery 21, 1580-1587.

46. Itoi, E., Kuechle, D.K., Newman, S.R., Morrey, B.F., An, K.N., 1993. Stabilizing function of the biceps in stable and unstable shoulders. Journal of Bone and Joint Surgery (British) 75, 546-550.

47. Pagnani, M.J., Deng, X.H., Warren, R.F., Torzilli, P.A., 1994. Effect of the long head of the biceps and superior labral lesions on glenohumeral translation. Trans Orthopaedic Research Society 19, 649-650.

48. Rodosky, M.W., Harnerm C.D., Fu, F.H., 1994. The role of the long head of the biceps muscle and superior glenoid labrum in anterior stability of the shoulder. American Journal of Sports Medicine 22, 121-130.

49. Youm, T.E.l., Attrache, N.S., Tibone, J.E., McGarry, M.H., Lee, T.Q., 2009. The effect of the long head of the biceps on glenohumeral kinematics. Journal of Shoulder and Elbow Surgery 18, 122-129.

50. McMahon, P.J., Burkart, A., Musahl, V., Debski, R.E, 2004. Glenohumeral translations are increased after a type II superior labrum anterior- posterior lesion: a cadaveric study of severity of passive stabilizer injury. Journal of Shoulder and Elbow Surgery 13, 39-44.

51. Burns, J.P., Bahk, M., Snyder, S.J., 2011. Superior labral tears: repair versus biceps tenodesis. Journal of Shoulder Elbow Surgery 20, S2

52. Anderson, A.E., Ellis, B.J., Maas, S.A., Weiss, J.A., 2010. Effects of idealized joint geometry on finite element predictions of cartilage contact stresses in the hip. Journal of Biomechanics 43, 1351-1357.

53. Adams, C.R., Baldwin, M.A., Laz, P.J., Rullkoetter, P.J., Langenderfer, J.E., 2007. Effects of rotator cuff tears on muscle moment arms: A computational study. Journal of Biomechanics 40, 3373-3380.

54. Clavert, P., Zerah, M., Krier, J., Mille, P., Kempf, J.F., Kahn, J.L., 2006. Finite element analysis of the strain distribution in the humeral head tubercles during abduction: comparison of young and osteoporotic bone. Surgical and Radiologic Anatomy 28, 581–587.

55. Ellis, B.J., Debski, R.E., Moore, S.M., McMahon, P.J., Weiss, J.A., 2007. Methodology and sensitivity studies for finite element modeling of the inferior glenohumeral ligament complex. Journal of Biomechanics 40, 603–612.

56. Ramos, A., Simoes, J.A., 2006. Tetrahedral versus hexahedral finite elements in numerical modelling of the proximal femur. Medical Engineering and Physics 28, 916–924.

57. Weiss, J. A., Gardiner, J.C., Ellis, B.J., Lujan, T.J., Phatak, N.S., 2005. Three-dimensional finite element modeling of ligaments: technical aspects. Medical Engineering and Physics 27, 845– 861.

58. Erdemir, A., Guess, T.M., Halloran, J., Tadepalli, S.C., Morrison, T.M., 2012. Considerations for reporting finite element analysis studies in biomechanics. Journal of Biomechanics 45, 625-633.

59. Yao, J., Snibbe, J., Maloney, M., Lerner, A.L., 2006. Stresses and strains in the medial meniscus of an ACL deficient knee under anterior loading: a finite element analysis with image-based experimental validation. Journal of Biomechanical Engineering 128, 135-141.

60. Henak, C.R., Ellis, B.J., Harris, M.D., Anderson, A.E., Peters, C.L., Weiss, J.A., 2011. Role of the acetabular labrum in load support across the hip joint. Journal of Biomechanics 44, 2201-2206.

61. Carpenter, J.E., Wening, J.D., Mell, A.G., Langenderfer, J.E., Kuhn, J.E., Hughes, R.E., 2005. Changes in the long head of the biceps tendon in rotator cuff tear shoulders. Clinical Biomechanics 20, 162-165.

62. McGough, R.L., Debski, R.E., Taskiran, E., Fu, F.H., Woo, S.L., 1996. Mechanical properties of the long head of the biceps tendon. Knee Surgery Sports Traumatology Arthroscopy 3, 226-229.

63. Angllin, C., Tolhurst, P., Wyss, U.P., Pichora, D.R., 1999. Glenoid cancellous bone strength and modulus. Journal of Biomechanics 32, 1091-1097.

64. Cooper, D. E., Arnoczky, S. P., O'Brien, S. J., Warren, R. F., DiCarlo, E., Allen, A. A., 1992, "Anatomy, histology, and vascularity of the glenoid labrum. An anatomical study," Journal of Bone and Joint Surgery (American) 74, 46-52.

65. Nishida, K., Hashizume, H., Toda, K., Inoue, H., 1996. Histologic and scanning electron microscopic study of the glenoid labrum. Journal of Shoulder and Elbow Surgery 5, 132–138.

66. Weinans, H., Huiskes, R., Grootenboer, H.J., 1992. The behavior of adaptive bone-remodeling simulation models. Journal of Biomechanics 25, 1425-1441.

67. Carter, D.R., Orr, T.E., 1992. Skeletal development and bone functional adaptation. Journal of Bone and Mineral Research 7, S389-S395.

68. Huiskes, R., Weinnans, H., Grootenboer, H.J., Dalstra, M., Fudala, B., Slooff, T.J., 1987. Adaptive bone-remodeling theory applied to prosthetic-design analysis. Journal of Biomechanics 20, 1135-1150.

69. An, K.N., Hu, F.C., Morrey, B.F., Linscheid, R.L., Chao, E.Y., 1981. Muscles across the elbow joint: A biomechanical analysis. Journal of Biomechanics 14, 659-669.

70. Murray, W.M., Buchanan, T.S., Delp, S.L., 2000. The isometric functional capacity of muscles that cross the elbow. Journal of Biomechanics 33, 943-952.

71. Bassett, R.W., Browne, A.O., Morrey, B.F., An, K.N., 1990. Glenohumeral muscle force and moment mechanics in a position of shoulder instability. Journal of Biomechanics 23, 405-415.

72. Alexander, R.M., Vernon, A., 1975. The dimension of knee and ankle muscles and the forces they exert. Journal of Human Movement Studies 1, 115-123.

73. Sacks, R.D., Roy, R.R., 1982. Architecture of the hind limb muscles of cats: Functional significance. Journal of Morphology, 185-195.

74. Maganaris, C.N., Baltzopoulos, V., 2000. In vivo mechanics of maximum isometric muscle contraction in man: Implications for modelling-based estimates of muscle specific tension. In Herzog W. (Ed). Skeletal muscle mechanics: from mechanisms to function. Wiley & Sons Ltd, 267-288.

75. Ikai, M, Fukunaga, T., 1968. Calculation of muscle strength per unit of cross sectional area of human muscle. Zeitschrift fur Angewandte Physiology und Einschlieblich Arbeit Physiology 26, 26.

76. Langenderfer, J., LaScalza, S., Mell, A., Carpenter, J.E., Kuhn, K.E., Hughes, R.E., 2005. An EMB-driven model of the upper extremity and estimation of long head biceps force. Computers in Biology and Medicine 35, 25-39.

77. Doherty, T.J., 2001. The influence of aging and sex on skeletal muscle mass and strength. Nutrition and Physiological Function 4, 503-508.

78. Klitgaard, H., Mantoni, M., Schiaffino, S., 1990. Function, morphology and protein expression of ageing skeletal muscle: A cross sectional study of elderly men with different training backgrounds. Acta Physiologica Scandinavica 140, 41-54.

79. Rice, C.L., Cunningham, D.A., Paterson, D.H., Lefcoe, M.S., 1989. Arm and leg compositon determined by computed tomography in young and elderly men. Clinical Physiology 9, 207-220.

80. Mura, N., O'Driscoll, S.W., Zobitz, M.E., Heers, G., Jenkyn, T.R., Chou, S.M., Halder, A.M., An, K.N., 2003. The effect of infraspinatus disruption on glenohumeral torque and superior migration of the humeral head: a biomechanical study. Journal of Shoulder and Elbow Surgery 12, 179-184.

81. Kaneko, K., De Mouy, E.H., Brunet, M.E., 1995. Massive rotator cuff tears. Screening by routine radiographs. Clinical Imaging 19, 8-11.

82. Weiner, D.S., Macnab, I., 1970. Superior migration of the humeral head. A radiological aid in the diagnosis of tears of the rotator cuff. Journal of Bone and Joint Surgery (British) 52, 524-527.

83. Nam, E.K., Snyder, S.J., 2003. The diagnosis and treatment of superior labrum, anterior and posterior (SLAP) lesions. American Journal of Sports Medicine 31, 798-810.

84. Snyder, S.J., Karzel, R.P., Del Pizzo, W., 1990. SLAP lesions of the shoulder. Arthroscopy 6, 274-279.

85. Giphart, J.E., Elser, F., Cewing, C.B., Torry, M.R., Millett, P.J., 2012. The long head of the biceps tendon has minimal effect on in vivo glenohumeral kinematics: A biplane fluoroscopy study. American Journal of Sports Medicine 41, 202-212.

86. Pradhan, R.L., Itoi, E., Kido, T., Hatakeyama, Y., Urayama, M., Sato, K., 2000. Effects of biceps loading and arm rotation on the superior labrum in the cadaveric shoulder. Tohoku Journal of Experimental Medicine 190, 261-269.

87. Nakajima, T., Hughes, R.E., An, K.N., 2004; Effect of glenohumeral rotations and translations on supraspinatus tendon morphology. Clinical biomechanics 19, 579-585.

88. Warner, J.J.P., McMahon, P.J., 1995. The role of the long head of the biceps brachii in superior stability of the glenohumeral joint. Journal of Bone and Joint Surgery (American) 77, 366-372.

CHAPTER VI

SUMMARY

Summary

Despite numerous hypotheses and experiments on the injury mechanism of the superior shoulder labrum, SLAP lesion, the tear mechanism is not clearly understood. Therefore a controversy exists concerning the optimal treatment of a labral tear. In order to understand the effect of individual factors on both initiation and propagation of the SLAP tear, a finite element model was developed for this study. In this dissertation, the working hypothesis was that it is possible to use finite element models to explore the factors underlying the initiation and propagation of a SLAP lesion. This hypothesis is supported through Chapter II, III, and IV. .

Chapter II was designed to validate the extended finite element model by adding the biceps tendon to the study of the mechanism of tears in the superior labrum. The strong correlation of the finite element model with the experimental measures and consistency of predicted labral strains with superior labral pathology were demonstrated. The insensitivity of the labral strain pattern to the changes in material parameters provides strong potential for utilizing the finite element model to investigate the mechanism of the SLAP lesion.

Chapter III described a risk of injury to the superior glenoid labrum due to the superior translation of the humeral head, as can be seen in cases of rotator cuff tears, combined with tensile loading on the long head of the biceps tendon. Pathologic loading of the labrum was simulated, and the more significant effect of superior translation of the humeral head than the effect of biceps tension on the increasing the intact labral strain was observed. The predicted peak strain was lower than the failure strain suggesting that repetitive micro-trauma or tissue fatigue rather than a single loading event was the cause of a mid-substance failure of the labrum.

Chapter IV provided the investigation of the effect of the biceps tension on the propagation of the SLAP lesion by observing mechanical behavior of the torn superior labrum. An area of high strain in the torn labrum was found at the edge of each existing tear. The predicted labral strain was increased with increasing biceps tension regardless of the tear size. The stronger correlation between increasing biceps tension and increasing the strain was represented in the labrum having a larger SLAP tear than the span of the biceps attachment on the superior labrum. Since the impact of the biceps tension was more significant with the larger torn labrum than with the small torn labrum, the biceps tension was suggested as a critical factor in the propagation of existing SLAP lesions. In addition, the current SLAP tear size was suggested as one of the criteria to select the optimal treatment of SLAP tear.

In summary, the greater the superior displacement in the glenohumeral joint, the more at risk the superior labrum is for the initiation of a tear. Propagation of the tear will then occur under large muscle forces from the long head of the biceps. Once a large tear has developed, then the model shows that cutting a biceps tendon will reduce the risk for complete failure of the superior labrum. This work was the first study on both initiation and propagation of the SLAP

tear using the strain predicted by a validated first finite element model. However, findings in this study is a labrum centric interpretation.